Annals of Physics 481 (2025) 170143

Contents lists available at ScienceDirect

Annals of Physics

journal homepage: www.elsevier.com/locate/aop

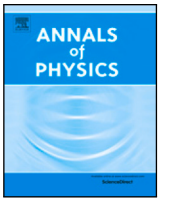

Entangling power for symmetric multiqubit systems: A geometrical approach

Eduardo Serrano-Ensástiga [a,*], Diego Morachis Galindo [a,b], Jesús A. Maytorena [b], Chryssomalis Chryssomalakos [c]

[a] Institut de Physique Nucléaire, Atomique et de Spectroscopie, CESAM, University of Liège, B-4000, Liège, Belgium
[b] Departamento de Física, Centro de Nanociencias y Nanotecnología, Universidad Nacional Autónoma de Mexico, Apartado Postal 14, 22800, Ensenada, Baja California, Mexico
[c] Instituto de Ciencias Nucleares, Universidad Nacional Autónoma de Mexico, PO Box 70-543, 04510, CDMX, Mexico

ARTICLE INFO

Keywords:
Unitary gates
Entangling power
Symmetric multipartite systems
Geometrical methods

ABSTRACT

Unitary gates with high entangling power are relevant for several quantum-enhanced technologies due to their entangling capabilities. For symmetric multiqubit systems, such as spin states or bosonic systems, the particle exchange symmetry restricts these gates and also the set of not-entangled states. In this work, we analyze the entangling power of unitary gates in these systems by reformulating it as an inner product between vectors with components given by SU(2) invariants. For small number of qubits, this approach allows us to study analytically the entangling power including the detection of the unitary gate that maximizes it. We observe that extremal unitary gates exhibit entanglement distributions with high rotational symmetry, same that are linked to a convex combination of Husimi functions of certain states. Furthermore, we explore the connection between entangling power and the Schmidt numbers admissible in some quantum state subspaces. Thus, the geometrical approach presented here suggests new paths for studying entangling power linked to other concepts in quantum information theory.

1. Introduction

Entanglement is a foundational concept in quantum theory and a vital resource for quantum technologies such as quantum computing, cryptography, metrology and simulation [1–3]. In multipartite quantum systems, it is generated through nonlocal unitary transformations, since local operations cannot alter the entanglement of a state [1]. It is therefore natural to investigate the entangling capacity of nonlocal unitary gates, and how to create highly entangled states via the evolution of nonlocal Hamiltonians or pulse sequences in physical systems [4–11]. On the theoretical side, several concepts have been proposed to assess the capability of unitary gates in generating quantum resources such as *gate typicality*, *disentangling power*, or *perfect entanglers* [12–15]. One of the most intuitively appealing quantities is the *entangling power* of a unitary gate [12] which is defined as the average entanglement generated by a unitary gate over the set of separable (not-entangled) states. Extensive studies of the entangling power have been carried out in bipartite systems [16–23] with generalizations to two-qubit global noise channels [24] and multipartite systems [25,26]. The entangling power of a unitary operator is also connected to its entanglement in its own Schmidt decomposition [16,27] or to invariant quantities under local transformations [8,28,29]. Furthermore, connections have been identified between highly entangling unitary gates and Quantum Error-Correcting Codes [25], absolutely maximally entangled

* Corresponding author.
E-mail addresses: ed.ensastiga@uliege.be (E. Serrano-Ensástiga), chryss@nucleares.unam.mx (C. Chryssomalakos).

https://doi.org/10.1016/j.aop.2025.170143
Received 22 January 2025; Accepted 26 June 2025
Available online 8 July 2025

(AME) states [26], unitary operators invariant under local actions of diagonal unitary and orthogonal groups [30], and quantum versions of chaotic systems [31–33].

When a multiqubit system is restricted to its symmetric subspace, the set of product states is significantly reduced to the set of Spin-Coherent (SC) states, which form a 2-sphere within the Hilbert space of quantum states [3,34]. Additionally, the local unitary transformations are limited to the global rotations, specifically global SU(2) transformations generated by the angular momentum operators. Symmetric multiqubit states arise in bosonic systems, such as two-mode multiphotonic systems or spin-j states. Moreover, the symmetric subspace of N qubit states is equivalent to the Hilbert space of spin-j ($j = N/2$) states, which makes the study of the entangling power of single spin states relevant in distinct physical platforms.

For the symmetric two-qubit case, which can be thought of as a spin-1 system, the entangling power of 3×3 unitary matrices has been studied in Ref. [35]. One key mathematical feature that arises in the study of those unitaries is the Cartan decomposition, which factorizes any quantum gate as a non-local operation multiplied on each side by local SU(2) transformations [36]. The entangling power of the unitary is encoded into the non-local factor, which is obtained by exponentiating the maximally commuting (Cartan) subalgebra of $\mathfrak{su}(3)$. This allows to represent the unitaries with equivalent entangling properties in an euclidean two-dimensional space [35]. For symmetric N-qubit systems with $N > 2$, the Cartan decomposition would not represent such a significant advantage, since the number of relevant parameters grows quadratically with the dimension of the system.

In this work, we study the entangling power of unitary transformations acting in symmetric multiqubit systems. We reformulate its original expression in terms of SU(2) invariant quantities of the unitary operators. This geometrical approach connects the entangling power to other well-known quantities in quantum information theory.

The structure of the paper is as follows: Section 2 considers symmetric multiqubit states and reviews, in this context, the formal definitions of the entropy of entanglement and of the entangling power — we derive the above mentioned geometric expression of the latter in Section 3. We then calculate the entangling power and the entanglement distribution on the sphere for systems with a small number of qubits in Sections 4 and 5, respectively, including the search of unitary gates with the best entangling capabilities. Section 6 contains the calculation of the average entangling power over all unitary gates. An interesting connection between entangling power and Schmidt numbers is explored in 7. We give some last remarks in Section 8.

2. Basic concepts

2.1. Equivalence between symmetric multiqubit states and spin-j states

We start this section by briefly describing the equivalence between the symmetric sector of N qubits and a spin $j = N/2$ state (see Ref. [37] for a detailed discussion of this equivalence). The symmetric sector of the N-qubit system is spanned, for instance, by the Dicke states $|D_k^{(N)}\rangle$

$$|D_k^{(N)}\rangle = K \sum_{\Pi} \Pi \left(\underbrace{|+\rangle \otimes \cdots \otimes |+\rangle}_{N-k} \otimes \underbrace{|-\rangle \otimes \cdots \otimes |-\rangle}_{k} \right), \tag{1}$$

where K is a normalization factor and the sum runs over all the permutations of the qubits. If we consider that the qubits are spins 1/2, the states $|D_k^{(N)}\rangle$ are eigenvectors of the angular momentum operators J_z and $\mathbf{J}^2 = J_x^2 + J_y^2 + J_z^2$

$$\begin{aligned} \mathbf{J}^2 |D_k^{(N)}\rangle &= j(j+1)|D_k^{(N)}\rangle, \\ J_z |D_k^{(N)}\rangle &= m|D_k^{(N)}\rangle. \end{aligned} \tag{2}$$

with $m = j - k$. Thus, the span of the Dicke states constitute a spin-j Hilbert space, denoted as $\mathcal{H}^{(j)}$, and where we can identify $|D_k^{(N)}\rangle = |j, m\rangle$. This space constitutes a spinor system because its elements transform under rotations with respect to the spin-j irreducible representation (irrep) of SU(2). From now on, we mostly work in the language of spins where the SU(2) irreps appear naturally.

2.2. Bipartite entanglement and entangling power

We consider a single spin-j (symmetric $N = 2j$-qubits) system with Hilbert space $\mathcal{H}^{(j)}$ and the Hilbert–Schmidt (HS) space of bounded operators $\mathcal{HS}(\mathcal{H}^{(j)})$ acting on $\mathcal{H}^{(j)}$. In this framework, we consider a bipartition of these $2j$ qubits $\mathcal{H}^{(j)} \subset \mathcal{H}_A \otimes \mathcal{H}_B$ and assume, without loss of generality, that $\dim(\mathcal{H}_A) \leqslant \dim(\mathcal{H}_B)$. Moreover, since any subsystem of a symmetric state is also symmetric, we can take as subsystems $\mathcal{H}_A \cong \mathcal{H}^{(q/2)}$ and $\mathcal{H}_B \cong \mathcal{H}^{(j-q/2)}$. In other words, the bipartition involves states of spins $q/2$ and $j - q/2$, respectively. The entanglement of a bipartite state $|\Psi\rangle \in \mathcal{H}_A \otimes \mathcal{H}_B$ can be quantified by the (normalized) linear entanglement entropy [12]

$$E(|\Psi\rangle) \equiv \frac{d}{d-1} \left[1 - \mathrm{Tr}\left(\rho_A^2\right) \right], \tag{3}$$

where $E(|\Psi\rangle) \in [0, 1]$, $\rho_A = \mathrm{Tr}_B(|\Psi\rangle\langle\Psi|)$ is the reduced mixed state after tracing out the subsystem B, and $d = \dim\left(\mathcal{H}_A\right)$. For a general bipartite pure state with Schmidt decomposition

$$|\Psi\rangle = \sum_{k=1}^{d} \sqrt{\Gamma_k} |\psi_{A,k}\rangle \otimes |\psi_{B,k}\rangle, \tag{4}$$

where $\{|\psi_{A,k}\rangle\}_k \subset \mathcal{H}_A$ and $\{|\psi_{B,k}\rangle\}_k \subset \mathcal{H}_B$ are orthogonal sets of states and $\sum_k \Gamma_k = 1$, we have

$$E(|\Psi\rangle) = \frac{d}{d-1}\left[1 - \sum_{k=1}^{d} \Gamma_k^2\right]. \tag{5}$$

In particular, $E(|\Psi\rangle) = 0$ for bipartite product states $|\Psi\rangle = |\psi_A\rangle \otimes |\psi_B\rangle$. On the other hand, the maximally entangled states have Schmidt numbers $\Gamma_k = 1/\sqrt{d}$ and $E(|\Psi\rangle) = 1$. Each bipartition with $q \leq \lfloor j \rfloor$ defines a different measure of entanglement E_q. This because $\mathrm{Tr}(\rho_A^2) = \mathrm{Tr}(\rho_B^2)$, and thus measures of entanglement E_q for $q > \lfloor j \rfloor$ are linear combinations of those of lower q values.

The product (separable) states in $\mathcal{H}^{(j)}$, for any bipartition, are the spin-coherent (SC) states $|j, \mathbf{n}\rangle \equiv D^{(j)}(\mathbf{n})|j, j\rangle$ which constitute a 2-sphere in $\mathcal{H}^{(j)}$ [34]. A possible parametrization of them is given by the rotations $D^{(j)}(\mathbf{n}) = D^{(j)}(0, \theta, \phi)$ which align the $\mathbf{z}$ axis to the direction $\mathbf{n}$ with spherical angles (θ, ϕ). $D^{(j)}(\alpha, \beta, \gamma)$ denotes the irreducible representation j (j-irrep) of a rotation matrix in the Euler angle parametrization [38]. The *entangling power* of a quantum unitary gate $U \in \mathcal{HS}(\mathcal{H}^{(j)})$, with respect to E_q, is defined as the average entanglement produced by U acting on the SC states [12],

$$e_{\mathrm{p}}(E_q, U) \equiv \overline{E_q(U|j, \mathbf{n}\rangle)} = \frac{1}{4\pi}\int_{S^2} E_q(U|j, \mathbf{n}\rangle)\mathrm{d}\mathbf{n}. \tag{6}$$

It is easily seen that

$$e_{\mathrm{p}}\left(E_q, R_1 U R_2\right) = e_{\mathrm{p}}(E_q, U), \tag{7}$$

for all q, where $R_{1,2}$ are matrices representing arbitrary SU(2) elements. If U itself is an SU(2) element, then $e_{\mathrm{p}}(E_q, U) = 0$ for all q.

Lastly, and since we will use for our main results, we specify the coupled basis of two spins

$$|j_1, j_2, L, M\rangle \equiv \sum_{m_2=-j_2}^{j_2} \sum_{m_1=-j_1}^{j_1} C^{LM}_{j_1 m_1 j_2 m_2} |j_1, m_1\rangle |j_2, m_2\rangle, \tag{8}$$

with $|j_1, m_1\rangle|j_2, m_2\rangle = |j_1, m_1\rangle \otimes |j_2, m_2\rangle$, and $C^{LM}_{j_1 m_1 j_2 m_2}$ denoting the Clebsch–Gordan coefficients.

2.3. Case $j = 1$ ($N = 2$)

For a generic unitary matrix $U \in \mathrm{SU}(3)$, the entangling power $e_{\mathrm{p}}(E_q, U)$ for $j = 1$ and $q = 1$ can be written as [35]

$$e_{\mathrm{p}}(E_1, U) = \frac{3}{5}\left(1 - \frac{1}{9}|\mathrm{Tr}\,(m)|^2\right), \tag{9}$$

where

$$\mathrm{Tr}(m) = \mathrm{Tr}(U_B^T U_B), \tag{10}$$

and U_B is the unitary matrix U transformed in the symmetric Bell states basis, $U_B = Q^\dagger U Q$[1] with

$$Q = \frac{1}{\sqrt{2}}\begin{pmatrix} 1 & 0 & i \\ 0 & i\sqrt{2} & 0 \\ 1 & 0 & -i \end{pmatrix}. \tag{11}$$

After some algebra, we can also write Eq. (10) as

$$\mathrm{Tr}(m) = \mathrm{Tr}\left(\Phi U^T \Phi U\right), \quad \text{with } \Phi = \begin{pmatrix} 0 & 0 & -1 \\ 0 & 1 & 0 \\ -1 & 0 & 0 \end{pmatrix}. \tag{12}$$

The unitary transformations of spin-1 states can be parametrized using the Cartan decomposition [35,36], with the SU(2) subgroup generated by the $j = 1$ angular momentum operators. A possible parametrization is $U = R_1 A R_2$ with $R_1, R_2 \in \mathrm{SU}(2)$ and

$$A = \begin{pmatrix} \frac{\lambda_1+\lambda_3}{2} & 0 & \frac{\lambda_1-\lambda_3}{2} \\ 0 & \lambda_2 & 0 \\ \frac{\lambda_1-\lambda_3}{2} & 0 & \frac{\lambda_1+\lambda_3}{2} \end{pmatrix}, \tag{13}$$

with

$$\lambda_1 = e^{\frac{i}{2}\left(-c_1+c_2+c_3\right)}, \qquad \lambda_2 = e^{\frac{i}{2}\left(c_1+c_2-c_3\right)}, \qquad \lambda_3 = e^{\frac{i}{2}\left(c_1-c_2+c_3\right)}, \tag{14}$$

and where the real parameters c_k fulfill $c_1 + c_2 + c_3 = 0$ [35]. Given that the entangling power is invariant under left and right rotations (see Eq. (7)), $e_{\mathrm{p}}(E_1, U)$ only depends on the c_i's,

$$e_{\mathrm{p}}(E_1, U) = \frac{4}{15}\left(\sin^2 c_{12} + \sin^2 c_{13} + \sin^2 c_{23}\right), \tag{15}$$

[1] Here, we consider the Q matrix of [35] in the symmetric subspace of $\mathcal{H}_{1/2}^{\otimes 2}$.

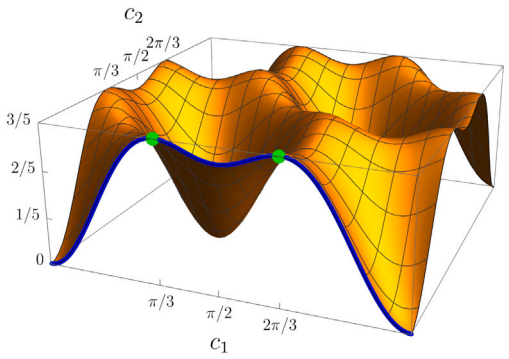

Fig. 1. Plot of the function $e_p(E_1, U)$ given in Eq. (15). One can clearly access a maximum with $c_2 = 0$ (blue curve). Two particular maxima are shown (green points); the one on the right, corresponding to $c_1 = 2\pi/3$, gives the U_0 in (16).

with $c_{ij} = c_i - c_j$. We plot $e_p(E_1, U)$ as a function of c_1 and c_2 in Fig. 1. For $c_2 = 0$, we observe two unitary matrices attaining the maximum at $c_1 = \pi/3$ and $2\pi/3$, respectively. The latter solution has corresponding unitary matrix (with $R_{1,2} = I$)

$$U_0 = \begin{pmatrix} \frac{1}{2}(\omega+1) & 0 & \frac{1}{2}(\omega-1) \\ 0 & \omega^{-1} & 0 \\ \frac{1}{2}(\omega-1) & 0 & \frac{1}{2}(\omega+1) \end{pmatrix}, \tag{16}$$

where $\omega = e^{-i\pi/3}$ is a cubic root of -1 and $e_p(E_1, U_0) = 3/5$. One can find two rotations to construct another unitary gate $U_0' = R_1 U_0 R_2$ with the same entangling power as U_0 but consisting simply of a permutation matrix

$$U_0' = \begin{pmatrix} 1 & 0 & 0 \\ 0 & 0 & 1 \\ 0 & 1 & 0 \end{pmatrix}. \tag{17}$$

3. Entangling power for symmetric $N = 2j$ qubits

Our first result is the reformulation of $E_q(U|j, \mathbf{n}\rangle)$ for a general $U \in \mathrm{SU}(N+1)$ in the form

$$E_q(U|j, \mathbf{n}\rangle) = 1 - \langle 2j, \mathbf{n}|\mathcal{U}^\dagger \mathcal{M}_q \mathcal{U}|2j, \mathbf{n}\rangle, \tag{18}$$

where $\mathcal{U} \equiv U \otimes U$ and

$$\mathcal{M}_q \equiv \frac{q+1}{q} \sum_{L=0}^{2j} (-1)^{2j+L} \chi(q, j, L) \mathcal{P}_L, \tag{19}$$

with $\mathcal{U}, \mathcal{M}_q \in \mathcal{HS}(\mathcal{H}^{(j)\otimes 2})$,

$$\chi(q, j, L) \equiv \sum_{\sigma=1}^{q} (2\sigma+1) \frac{\begin{Bmatrix} q/2 & q/2 & q \\ q/2 & q/2 & \sigma \end{Bmatrix} \begin{Bmatrix} j & j & L \\ j & j & \sigma \end{Bmatrix}}{\begin{Bmatrix} j & j & 2j \\ j & j & \sigma \end{Bmatrix}} \tag{20}$$

and

$$\mathcal{P}_L \equiv \sum_{M=-L}^{L} |j, j, L, M\rangle\langle j, j, L, M|. \tag{21}$$

Here, the curly bracket represents the Wigner 6-j symbol [38]. $\mathcal{P}_L$ is the projector operator in the subspace of $\mathcal{H}^{(j)\otimes 2}$ defined with the states of coupled basis (8) with total angular momentum L. The derivation of Eq. (18) is given in Appendix A. We now use the resolution of unity of the SC states [39],

$$\frac{1}{4\pi} \int |2j, \mathbf{n}\rangle\langle 2j, \mathbf{n}| \mathrm{d}\mathbf{n} = \frac{\mathcal{P}_{2j}}{4j+1} \equiv \mathcal{N}, \tag{22}$$

to calculate e_p, yielding

$$e_p(E_q, U) = 1 - \mathrm{Tr}\left(\mathcal{U}\mathcal{N}\mathcal{U}^\dagger \mathcal{M}_q\right). \tag{23}$$

The fact that both operators $\mathcal{N}$ and $\mathcal{M}_q$ are linear combinations of $\mathcal{P}_L$'s, which are orthogonal among themselves, $\mathrm{Tr}(\mathcal{P}_L\mathcal{P}_K) = (2L+1)\delta_{LK}$, suggests a further reformulation of the e_{p}. Indeed, to an operator $V \in \mathcal{HS}(\mathcal{H}^{(j)\otimes 2})$, we associate the $(2j+1)$-dimensional vector $\overrightarrow{V}$ with SU(2)-invariant components,

$$\overrightarrow{V} = \left(\mathrm{Tr}\left(V\tilde{\mathcal{P}}_0\right), \ldots, \mathrm{Tr}\left(V\tilde{\mathcal{P}}_L\right), \ldots, \mathrm{Tr}\left(V\tilde{\mathcal{P}}_{2j}\right)\right), \tag{24}$$

where $\tilde{\mathcal{P}}_L = \mathcal{P}_L/\sqrt{2L+1}$. We obtain that

$$\left\langle \widehat{\mathcal{U}}\overrightarrow{\mathcal{N}}, \overrightarrow{\mathcal{M}}_q \right\rangle = \mathrm{Tr}\left(\mathcal{U}\mathcal{N}\mathcal{U}^\dagger\mathcal{M}_q\right), \tag{25}$$

where $\langle\cdot,\cdot\rangle$ is the euclidean inner product,

$$\left\langle \overrightarrow{V}, \overrightarrow{W} \right\rangle \equiv \sum_{k=0}^{2j} V_k W_k, \tag{26}$$

and $\widehat{\mathcal{U}}$ is a $(2j+1)\times(2j+1)$ real matrix with entries

$$\left(\widehat{\mathcal{U}}\right)_{mn} = \mathrm{Tr}\left(\mathcal{U}\tilde{\mathcal{P}}_m\mathcal{U}^\dagger\tilde{\mathcal{P}}_n\right). \tag{27}$$

Therefore, the entangling power reads

$$e_{\mathrm{p}}(E_q, U) = 1 - \left\langle \widehat{\mathcal{U}}\overrightarrow{\mathcal{N}}, \overrightarrow{\mathcal{M}}_q \right\rangle. \tag{28}$$

From Eqs. (26) and (27), we deduce that $\left\langle \widehat{\mathcal{U}}\overrightarrow{\mathcal{N}}, \overrightarrow{\mathcal{M}}_q \right\rangle = \left\langle \overrightarrow{\mathcal{N}}, \widehat{\mathcal{U}}^T\overrightarrow{\mathcal{M}}_q \right\rangle$. To summarize, we have expressed $e_{\mathrm{p}}(E_q, U)$ in terms of the euclidean inner product of two vectors, with components given by SU(2)-invariant quantities of the operators $\mathcal{N}$ and $\mathcal{M}_q$, one of them transformed by the unitary transformation $\mathcal{U}$. A similar formula for e_{p}, in terms of operators associated to the multipole operators [38], is given in Appendix B.

The projectors $\mathcal{P}_L$ change by a $(-1)^{2j+L}$ sign under particle exchange in $\mathcal{H}^{(j)\otimes 2}$. Since the unitary operators $\mathcal{U} = U \otimes U$ preserve this symmetry, $\mathrm{Tr}(\mathcal{U}\mathcal{P}_{2j}\mathcal{U}^\dagger\mathcal{P}_L)$ vanishes unless $L \equiv 2j \pmod 2$. Thus, the vector $\overrightarrow{\mathcal{N}} = (0, 0, \ldots, 1/\sqrt{4j+1})$ after a $\mathcal{U}$ transformation has components

$$\begin{aligned} &\left(0, \mathrm{Tr}\left(\mathcal{N}\tilde{\mathcal{P}}_1\right), 0, \mathrm{Tr}\left(\mathcal{N}\tilde{\mathcal{P}}_3\right), 0, \ldots, \mathrm{Tr}\left(\mathcal{N}\tilde{\mathcal{P}}_{2j}\right)\right), \\ &\left(\mathrm{Tr}\left(\mathcal{N}\tilde{\mathcal{P}}_0\right), 0, \mathrm{Tr}\left(\mathcal{N}\tilde{\mathcal{P}}_2\right), 0, \ldots, \mathrm{Tr}\left(\mathcal{N}\tilde{\mathcal{P}}_{2j}\right)\right), \end{aligned} \tag{29}$$

for $2j$ odd or even, respectively. On the other hand, $\overrightarrow{\mathcal{M}}_q$ has components for L both odd and even. As an example, the components of $\overrightarrow{\mathcal{M}}_1$ are

$$\left(\overrightarrow{\mathcal{M}}_1\right)_L = \frac{L(L+1) - 2j(j+1)}{2j^2}. \tag{30}$$

Nevertheless, the relevant components of $\mathcal{M}_q$ for e_{p} are the ones in common with $\widehat{\mathcal{U}}\overrightarrow{N}$ (29), *i.e.* , with $2j \equiv L \pmod 2$. These components of $\overrightarrow{\mathcal{N}}$ and $\overrightarrow{\mathcal{M}}_q$ lie in a hyperplane after any unitary transformation $\mathcal{U} = U \otimes U$ (see Identity 3 of Appendix C)

$$\begin{aligned} \sum_{\substack{L=0 \\ 2j\equiv L \pmod 2}}^{2j} \sqrt{2L+1}\left(\widehat{\mathcal{U}}\overrightarrow{\mathcal{N}}\right)_L &= \sum_{\substack{L=0 \\ 2j\equiv L \pmod 2}}^{2j} \mathrm{Tr}\left(\mathcal{U}\mathcal{P}_L\mathcal{U}^\dagger\mathcal{N}\right) = 1, \\ \sum_{\substack{L=0 \\ 2j\equiv L \pmod 2}}^{2j} \sqrt{2L+1}\left(\widehat{\mathcal{U}}\overrightarrow{\mathcal{M}}_q\right)_L &= \frac{(j+1)(2j+1)}{2j+1-q}. \end{aligned} \tag{31}$$

The components of $\overrightarrow{\mathcal{M}}_q$ for several spin values are shown in Table 1 — they satisfy the inequalities

$$0 \leqslant \mathrm{Tr}\left(\mathcal{U}\mathcal{P}_L\mathcal{U}^\dagger\mathcal{P}_K\right) \leqslant \min\left(2L+1, 2K+1\right), \tag{32}$$

for $L \equiv K \pmod 2$. This becomes evident if we take into account that the operators $\mathcal{P}_L$ and $\mathcal{P}_K$ project onto subspaces of dimensions $2L+1$ and $2K+1$, respectively. The unitary operator transforms this subspace while preserving its dimension. The trace in (32) then is just the projection of one of the subspaces, transformed by $\mathcal{U}$, onto the other. These inequalities can be used to find bounds for the components of the vector

$$p_L \equiv \left(\widehat{\mathcal{U}}\overrightarrow{\mathcal{N}}\right)_L, \qquad 0 \leqslant p_L \leqslant \frac{\sqrt{2L+1}}{4j+1}. \tag{33}$$

A unitary operator $\mathcal{U}$ that achieves a critical value of $e_{\mathrm{p}}(E_q, U)$ must fulfill

$$\mathrm{Tr}\left(\mathcal{U}\mathcal{N}\mathcal{U}^\dagger\left[\mathcal{M}_q, \mathcal{G}_a\right]\right) = 0, \quad \mathcal{G}_a = \mathbb{1}\otimes G_a + G_a \otimes \mathbb{1}, \tag{34}$$

Table 1
Vectors of SU(2) invariants of $\mathcal{M}_q$ (19) for the spin values $j = 1, 3/2, 2, 5/2$ and $q = 1, \dots, \lfloor j \rfloor$.

j	q	$\overrightarrow{\mathcal{M}}_q$
1	1	$\left(-2, -\sqrt{3}, \sqrt{5}\right)$
3/2	1	$\left(-\frac{5}{3}, -\frac{11}{3\sqrt{3}}, -\frac{\sqrt{5}}{3}, \sqrt{7}\right)$
2	1	$\left(-\frac{3}{2}, -\frac{5\sqrt{3}}{4}, -\frac{3\sqrt{5}}{4}, 0, 3\right)$
	2	$\left(-\frac{1}{4}, -\frac{\sqrt{3}}{2}, -\frac{3\sqrt{5}}{4}, -\frac{\sqrt{7}}{2}, 3\right)$
5/2	1	$\left(-\frac{7}{5}, -\frac{31\sqrt{3}}{25}, -\frac{23}{5\sqrt{5}}, -\frac{11\sqrt{7}}{25}, \frac{3}{5}, \sqrt{11}\right)$
	2	$\left(-\frac{7}{20}, -\frac{47\sqrt{3}}{100}, -\frac{31}{10\sqrt{5}}, -\frac{31\sqrt{7}}{50}, -\frac{3}{5}, \sqrt{11}\right)$

for any generator of the Lie algebra $G_a \in \mathfrak{su}(2j+1)$. If it satisfies additionally that the Hessian of e_{p} evaluated at $\mathcal{U}$,

$$H_{ab} \equiv -\mathrm{Tr}\left(\mathcal{U}\mathcal{N}\mathcal{U}^{\dagger}\left[\left[\mathcal{M}_q, \mathcal{G}_a\right], \mathcal{G}_b\right]\right), \tag{35}$$

has only negative eigenvalues, then $\mathcal{U}$ is a local maximum. Due to the invariance of $e_{\mathrm{p}}(E_q, U)$ under left and right SU(2) operations (7), at least 6 eigenvalues of H are equal to zero.

4. e_{p} for small number of qubits

4.1. $N = 2$ $(j = 1)$

We calculate again $e_{\mathrm{p}}(E_1, U)$ for $j = 1$ using the formulation given in the previous section. In this case, $\widehat{\mathcal{U}}\overrightarrow{\mathcal{N}} = (p_0, 0, p_2)$. The restriction to the hyperplane (31), $p_0 + \sqrt{5}p_2 = 1$, lets us write e_{p} in terms of only p_0,

$$e_{\mathrm{p}}(E_1, U) = 1 - \left\langle \widehat{\mathcal{U}}\overrightarrow{\mathcal{N}}, \overrightarrow{\mathcal{M}}_1 \right\rangle = 3p_0 \tag{36}$$

We recover (9) by calculating p_0,

$$\begin{aligned} 5p_0 =& \mathrm{Tr}\left(\mathcal{U}\mathcal{P}_2\mathcal{U}^{\dagger}\mathcal{P}_0\right) \\ =& \mathrm{Tr}\left(\mathcal{U}(\mathbb{1} - \mathcal{P}_0 - \mathcal{P}_1)\mathcal{U}^{\dagger}\mathcal{P}_0\right) \\ =& 1 - \mathrm{Tr}\left(\mathcal{U}\mathcal{P}_0\mathcal{U}^{\dagger}\mathcal{P}_0\right). \end{aligned} \tag{37}$$

Since $\mathcal{P}_0$ is a rank one operator, the last expression can be rewritten as

$$5p_0 = 1 - \left|\mathrm{Tr}\left(\mathcal{P}_0\mathcal{U}\right)\right|^2 = 1 - \frac{1}{9}\left|\mathrm{Tr}\left(\boldsymbol{\Phi}U^T\boldsymbol{\Phi}U\right)\right|^2, \tag{38}$$

where $\boldsymbol{\Phi}$ is defined in Eq. (12) and the last equality is derived as follows

$$\begin{aligned} \mathrm{Tr}(\mathcal{P}_0\mathcal{U}) =& \sum_{\substack{m_1 m_2 \\ n_1 n_2}} C^{00}_{1m_1 1m_2} C^{00}_{1n_1 1n_2} U_{m_1 n_1} U_{m_2 n_2} \\ =& \frac{1}{3}\sum_{m_1 n_1} (-1)^{m_1+n_1} U_{m_1 n_1} U_{-m_1 -n_1} \\ =& \frac{1}{3}\mathrm{Tr}\left(\boldsymbol{\Phi}U^T\boldsymbol{\Phi}U\right). \end{aligned} \tag{39}$$

We obtain the upper bound $e_{\mathrm{p}}(E_1, U) \leqslant 3/5$ from Eq. (33) — the inequality is in fact saturated by U_0 (16). In Fig. 2 (left frame) we plot the vectors $\widehat{\mathcal{U}}\overrightarrow{\mathcal{N}}$ for random unitary operators, produced with the Haar measure, as well as the vector $\widehat{\mathcal{U}}_0\overrightarrow{\mathcal{N}}$ with U_0 given by (16). We also plot the orthogonal complement $\overrightarrow{M}_q^{\perp}$ of $\overrightarrow{M}_q$ with respect to the inner product (26). As expected, $\mathcal{U}_0$ meets the criteria for a local maximum (34)–(35), with the Hessian there having two eigenvalues equal to −4 and six equal to 0.

4.2. $N = 3$ $(j = 3/2)$

The vector $\widehat{\mathcal{U}}\overrightarrow{\mathcal{N}} = (0, p_1, 0, p_3)$ is restricted in the hyperplane (31) $\sqrt{3}p_1 + \sqrt{7}p_3 = 1$. Hence, $e_{\mathrm{p}}(E_1, U)$ is also a function of one SU(2) invariant for $j = 3/2$,

$$e_{\mathrm{p}}(E_1, U) = \frac{20\sqrt{3}}{9}p_1 \leqslant \frac{20}{21}. \tag{40}$$

The bound is saturated by the unitary operator

$$U_0 = \begin{pmatrix} 0 & 1 & 0 & 0 \\ 0 & 0 & 0 & i \\ i & 0 & 0 & 0 \\ 0 & 0 & 1 & 0 \end{pmatrix}, \tag{41}$$

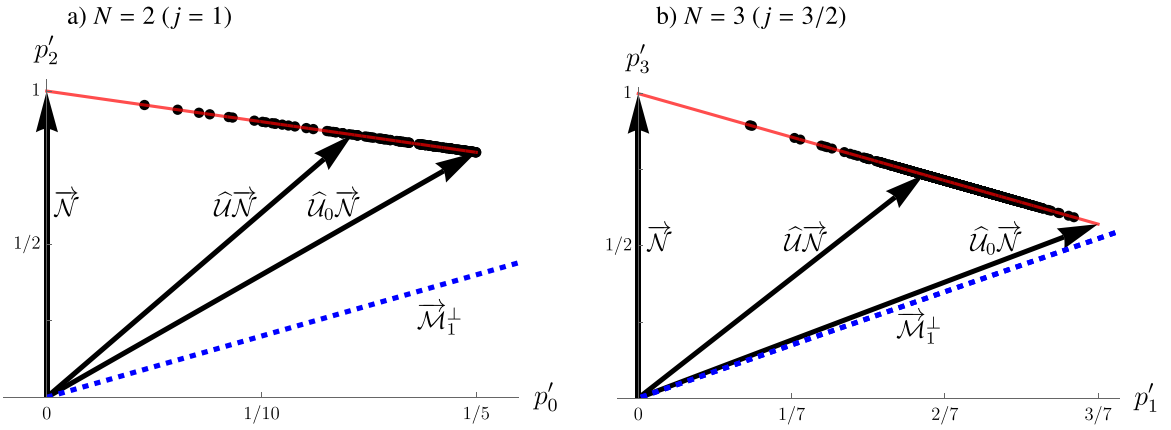

Fig. 2. Vectors of SU(2) invariants in the plane where $\widehat{\mathcal{U}}\vec{\mathcal{N}}$ has non-zero components (29) for (a) $N = 2$ and (b) $N = 3$. The black dots are the vectors corresponding to random, according to the Haar measure, unitary operators. The solid red segment is the part of the hyperplane (31) that also satisfies (33). The contour lines of $e_{\mathrm{p}}(E_1, U)$ are parallel to the dashed blue line representing $\vec{\mathcal{M}}_1^{\perp}$. The entangling power of U increases as the euclidean distance from $\widehat{\mathcal{U}}\vec{\mathcal{N}}$ to $\vec{\mathcal{M}}_1^{\perp}$ decreases. The upper bounds are saturated for the unitary transformations (16) (also (17)) for $N = 2$ and (41), for $N = 3$. To simplify the axes labels, we use the scaled variables $p'_\sigma = \sqrt{2\sigma+1}\,p_\sigma$.

which we identified as outlined in Section 7. Note that, in order to simplify the notation, we denote the optimal entangles by U_0 for all values of spin — which unitary operator is involved should be clear from the context. We plot the vectors $\widehat{\mathcal{U}}\vec{\mathcal{N}}$ for random unitary operators, as well as $\widehat{\mathcal{U}}_0\vec{\mathcal{N}}$ and $\vec{\mathcal{M}}_q^{\perp}$ in Fig. 2 (right frame). Again, it is verified that U_0 is a critical value of e_{p} with Hessian having eigenvalues equal to -8, $-8/5$ and 0, with degeneracies 4, 5 and 6, respectively.

4.3. $N = 4$ $(j = 2)$

Here, we have three different non-zero components in $\widehat{\mathcal{U}}\vec{N} = (p_0, 0, p_2, 0, p_4)$ restricted to the plane $p_0 + \sqrt{5}p_2 + 3p_4 = 1$, and two different non-equivalent bipartite entanglements

$$e_{\mathrm{p}}(E_q, U) = \frac{1}{4}\left(\frac{10p_0}{q} + 7\sqrt{5}p_2\right), \tag{42}$$

for $q = 1, 2$. Unlike the previous cases, the inequalities (33) provide a trivial bound for $e_{\mathrm{p}}(E_q, U)$. Through numerical search, we identified unitary matrices $U_0^{(q)}$ that we conjecture are optimal entanglers for E_q, $q = 1, 2$. They read

$$U_0^{(1)} = \begin{pmatrix} \beta\cos\alpha & 0 & 0 & 0 & i\beta\sin\alpha \\ 0 & e^{i\frac{\pi}{4}} & 0 & 0 & 0 \\ 0 & 0 & \beta^2 & 0 & 0 \\ 0 & 0 & 0 & e^{-i\frac{\pi}{4}} & 0 \\ -i\beta\sin\alpha & 0 & 0 & 0 & -\beta\cos\alpha \end{pmatrix}, \tag{43}$$

with $\alpha = \arctan\left(\sqrt{83/53}\right)$ and $\beta = e^{-i\arctan\left(\sqrt{53/83}\right)}$, and

$$U_0^{(2)} = \begin{pmatrix} 0 & 0 & 0 & i & 0 \\ i & 0 & 0 & 0 & 0 \\ 0 & 0 & 1 & 0 & 0 \\ 0 & 0 & 0 & 0 & i \\ 0 & i & 0 & 0 & 0 \end{pmatrix}. \tag{44}$$

Both unitary matrices fulfill the criteria for local maximum (34) and (35) for their respective E_q, with entangling power

$$e_{\mathrm{p}}\left(E_1, U_0^{(1)}\right) = \frac{6889}{7140} \approx 0.9648\,, \qquad e_{\mathrm{p}}\left(E_2, U_0^{(2)}\right) = \frac{25}{28} \approx 0.8929\,. \tag{45}$$

As for the previous cases, we plot the vectors $\widehat{\mathcal{U}}\vec{\mathcal{N}}$, $\widehat{\mathcal{U}}_0^{(q)}\vec{\mathcal{N}}$ and $\vec{\mathcal{M}}_q^{\perp}$ in Fig. 3.

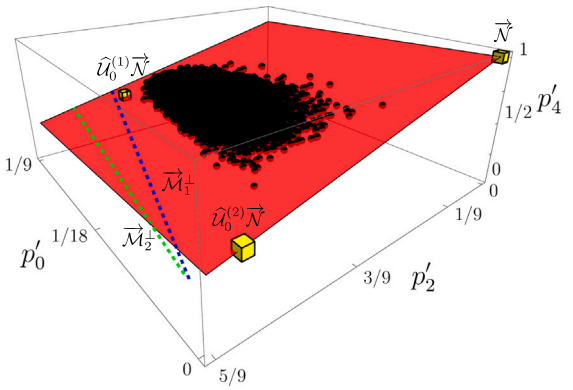

Fig. 3. Vectors $\widehat{\mathcal{U}}\overrightarrow{\mathcal{N}}$ for $j = 2$, where we plot only their non-zero components (29). The black dots are the vectors given by random unitary operators. The red plane is the restriction (31). The dashed blue and green lines denote the intersection of the red plane with $\overrightarrow{\mathcal{M}}_1^{\perp}$ and $\overrightarrow{\mathcal{M}}_2^{\perp}$, respectively. The yellow cubes represent the position of the vector $\overrightarrow{\mathcal{N}}$ and its corresponding transformed vector by the unitary operators $U_0^{(q)}$ given by Eqs. (43) and (44), respectively.

4.4. e_p of a unitary operator and its inverse

In this short section we comment on the relation between the entangling power of a unitary matrix U and its inverse. We find that, for $j = 1$ and $j = 3/2$, $e_{\rm p}(E_1, U) = e_{\rm p}(E_1, U^\dagger)$ for all $U \in {\rm SU}(2j+1)$. These results are derived from the expressions

$$\begin{aligned} e_{\rm p}(E_1,U) &= \frac{3}{5}\left[1 - {\rm Tr}\left(\mathcal{U}\mathcal{P}_0\mathcal{U}^\dagger\mathcal{P}_0\right)\right], \quad \text{for } j = 1, \\ e_{\rm p}(E_1,U) &= \frac{20}{63}\left[3 - {\rm Tr}\left(\mathcal{U}\mathcal{P}_1\mathcal{U}^\dagger\mathcal{P}_1\right)\right], \quad \text{for } j = 3/2, \end{aligned} \tag{46}$$

obtained from Eqs. (36)–(37) and Eq. (40), respectively. On the other hand, numerical calculations show that, in general, $e_{\rm p}(E_q, U) \neq e_{\rm p}(E_q, U^\dagger)$ for $j \geqslant 2$. In the case of $j = 2$, for instance, the $e_{\rm p}$ (42) can be rewritten as

$$36 e_{\rm p}(E_q,U) = -\frac{10}{q}{\rm Tr}\left(\mathcal{U}\mathcal{P}_2\mathcal{U}^\dagger\mathcal{P}_0\right) - 7{\rm Tr}\left(\mathcal{U}\mathcal{P}_0\mathcal{U}^\dagger\mathcal{P}_2\right) + \frac{10}{q}\left[1 - {\rm Tr}\left(\mathcal{U}\mathcal{P}_0\mathcal{U}^\dagger\mathcal{P}_0\right)\right] + 7\left[5 - {\rm Tr}\left(\mathcal{U}\mathcal{P}_2\mathcal{U}^\dagger\mathcal{P}_2\right)\right], \tag{47}$$

where the first two terms on the right-hand side provide the difference between $e_{\rm p}(E_q, U)$ and $e_{\rm p}(E_q, U^\dagger)$.

5. Entanglement distribution and husimi functions

Now we would like to study the entanglement $E_q(U|j,\mathbf{n}\rangle)$ as a function on the sphere where $\mathbf{n}$ lives. We start with the expression

$$E_q(U|j,\mathbf{n}\rangle) = 1 - \langle 2j,\mathbf{n}|\mathcal{D}_q(U)|2j,\mathbf{n}\rangle, \tag{48}$$

with

$$\mathcal{D}_q(U) \equiv \mathcal{P}_{2j}\mathcal{U}^\dagger\mathcal{M}_q\mathcal{U}\mathcal{P}_{2j}\,, \tag{49}$$

which follows from (18) since the state $|2j,\mathbf{n}\rangle$ lies in the subspace associated to $\mathcal{P}_{2j}$. The matrix $\mathcal{D}_q = \mathcal{D}_q(U)$ is Hermitian for any U and can be thought of as a $(4j+1)\times(4j+1)$ matrix when restricted to the image of $\mathcal{P}_{2j}$. Additionally, it rotates under SU(2) transformations as $D^{(2j)}(R)\mathcal{D}_q D^{(2j)\dagger}(R)$ with $D^{(2j)}(R)$ the $(2j)$-irrep of the rotation R. By Eq. (48), $E_q(U|j,\mathbf{n}\rangle)$ inherits the rotational symmetries of $\mathcal{D}_q$. These symmetries can be scrutinized by the Majorana representation for Hermitian operators [40]. In particular, we use it to verify the rotational symmetries of $E_q(U|j,\mathbf{n}\rangle)$ for the unitary gates mentioned below.

The eigendecomposition $\mathcal{D}_q = \sum_{k=1}^{4j+1}\sigma_k|\psi_k\rangle\langle\psi_k|$ also helps to recast the entanglement distribution on the sphere as

$$E_q(U|j,\boldsymbol{n}\rangle) = 1 - \sum_{k=1}^{4j+1}\sigma_k H_{|\psi_k\rangle}(\mathbf{n}), \tag{50}$$

with $H_{|\psi_k\rangle}(\mathbf{n}) = |\langle 2j,\mathbf{n}|\psi_k\rangle|^2$ being the Husimi function of $|\psi_k\rangle$ [39]. By averaging over the sphere, we find

$$\begin{aligned} e_{\rm p}(E_q,U) &= 1 - \sum_{k=1}^{4j+1}\sigma_k\overline{H_{|\psi_k\rangle}(\mathbf{n})} \\ &= 1 - \frac{1}{4j+1}\sum_{k=1}^{4j+1}\sigma_k \\ &= 1 - \frac{{\rm Tr}\left[\mathcal{D}_q(U)\right]}{4j+1}, \end{aligned} \tag{51}$$

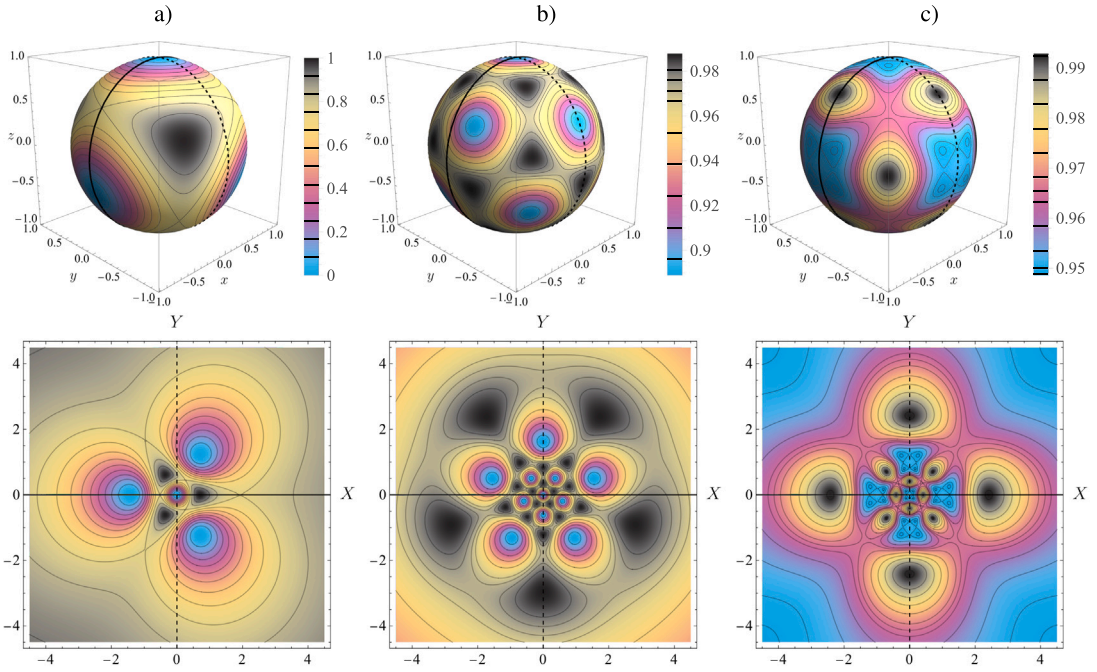

Fig. 4. Entanglement distribution $E_1(U|j,\mathbf{n}\rangle)$ (Top) and its stereographic projection (Bottom) obtained by the SC states after the action of the unitary operator (a) (17) (b) (41) and (c) (43) for the spin values $j = 1, 3/2, 2$, respectively. $E_q(U|\mathbf{n}\rangle)$ has tetrahedral, icosahedral and octahedral symmetry, respectively. These unitary operators maximize e_p for $j = 1, 3/2$, and apparently for $j = 2$, respectively. The numerical values of the contour lines are marked in each color bar.

which reduces to Eq. (28). Let us now study the entanglement distribution of the examples in Section 4.

5.1. $N = 2$ $(j = 1)$

We plot in Fig. 4a the entanglement distribution

$$E_1(U_0'|\mathbf{n}\rangle) = 4\sqrt{2}\sin^5\left(\frac{\theta}{2}\right)\cos^3\left(\frac{\theta}{2}\right)\cos(3\phi) + \frac{\sin^2\left(\frac{\theta}{2}\right)}{32}\left[90 + 105\cos(\theta) + 54\cos(2\theta) + 7\cos(3\theta)\right], \tag{52}$$

with U_0' defined in (17). Its corresponding matrix D_1 is equal to

$$D_1 = \begin{pmatrix} 1 & 0 & 0 & 0 & 0 \\ 0 & -1 & 0 & 0 & \sqrt{2} \\ 0 & 0 & 1 & 0 & 0 \\ 0 & 0 & 0 & 1 & 0 \\ 0 & \sqrt{2} & 0 & 0 & 0 \end{pmatrix}, \tag{53}$$

which exhibits tetrahedral symmetry. The same point group can be observed in the entanglement distribution of U_0' plotted in Fig. 4a. U_0' does not create any entanglement when applied to four SC states pointing in the vertices of a regular tetrahedron, one of which is $|\mathbf{z}\rangle$. On the other hand, it transforms the SC states pointing along the vertices of the antipodal tetrahedron into maximally entangled states. For instance, $U_0'|-\mathbf{z}\rangle = |1,0\rangle$. An alternative way to show the tetrahedral symmetry of the entanglement distribution is by direct calculation of the eigendecomposition of D_1

$$D_1 = \mathbb{1}_5 - 3|\psi_T\rangle\langle\psi_T|, \tag{54}$$

with

$$|\psi_T\rangle = -\sqrt{\frac{2}{3}}|2,1\rangle + \frac{1}{\sqrt{3}}|2,-2\rangle \tag{55}$$

a spin-2 state with tetrahedral symmetry [41]. By direct algebra, we obtain that

$$E_1(U_0', |1,\mathbf{n}\rangle) = 3H_{|\psi_T\rangle}(\mathbf{n}), \tag{56}$$

i.e. , the entanglement distribution of U_0' is proportional to the Husimi function of the tetrahedron state $|\psi_T\rangle$.

Similar expressions for $\mathcal{D}_1$ and E_1 are obtained for a general $U \in \mathrm{SU}(3)$ using the parametrization (13). By taking only the non-local term of the unitary gate $U = A$, we get that

$$\mathcal{D}_1 = \mathbb{1}_5 - \frac{4\Gamma_A}{3}|\psi_A\rangle\langle\psi_A|, \tag{57}$$

with

$$\Gamma_A = \sin^2 c_{12} + \sin^2 c_{13} + \sin^2 c_{23} \tag{58}$$

and

$$|\psi_A\rangle = \sqrt{\frac{3}{\Gamma_A}}\frac{\sin c_{12}}{2}\Big(|2,2\rangle + |2,-2\rangle\Big) + i\left(\frac{\cos c_{12} - e^{-i(c_{13}+c_{23})}}{\sqrt{2\Gamma_A}}\right)|2,0\rangle. \tag{59}$$

Thus,

$$E_1(U, |1,\mathbf{n}\rangle) = \frac{4\Gamma_A}{3}H_{|\psi_A\rangle}(\mathbf{n}), \tag{60}$$

with Γ_A proportional to $e_{\mathrm{p}}(E_1, U)$ (15).[2]

5.2. $N = 3$ $(j = 3/2)$

We now plot $E_1(U_0|3/2,\mathbf{n}\rangle)$, with U_0 the unitary transformation in (41), in Fig. 4b. The entanglement distribution

$$E_1(U_0|3/2,\mathbf{n}\rangle) = \frac{1}{1152}\left[1090 + 192\sin^5(\theta)\cos(\theta)\sin(5\phi)\ -15\cos(2\theta) - 18\cos(4\theta) - 33\cos(6\theta)\right] \tag{61}$$

has an icosahedral symmetry, and takes values in the interval $[8/9, 80/81]$. The rotational symmetries are also reflected in the configuration of the minima and maxima, which are arranged in an icosahedron and a dodecahedron, respectively. The corresponding $\mathcal{D}_1$ matrix has eigendecomposition given by

$$\mathcal{D}_1 = \mathbb{1}_7 - \frac{20}{9}\sum_{k=1}^{3}|\psi_k\rangle\langle\psi_k|, \tag{62}$$

with states[3]

$$|\psi_1\rangle = -i\sqrt{\frac{3}{5}}|3,2\rangle + \sqrt{\frac{2}{5}}|3,-3\rangle, \qquad |\psi_2\rangle = i\sqrt{\frac{2}{5}}|3,3\rangle + \sqrt{\frac{3}{5}}|3,-2\rangle, \qquad |\psi_3\rangle = |3,0\rangle. \tag{63}$$

The entanglement distribution is then given by

$$E_1(U_0|3/2,\mathbf{n}\rangle) = \frac{20}{9}\sum_{k=1}^{3}H_{|\psi_k\rangle}(\mathbf{n}). \tag{64}$$

5.3. $N = 4$ $(j = 2)$

We plot $E_1(U_0^{(1)}, |2,\mathbf{n}\rangle)$, with $U_0^{(1)}$ defined by (43), in Fig. 4c. We observe octahedral symmetry, confirmed by using the Majorana representation of mixed states [40]. In fact, the minima (maxima) of $E_1(U_0^{(1)}|2,\mathbf{n}\rangle)$ lie on the vertices of a truncated octahedron (cuboctahedron) — the explicit expression of this function is rather long and is not particularly enlightening. On the other hand, $E_2(U_0^{(2)}|2,\mathbf{n}\rangle)$, with $U_0^{(2)}$ as in Eq. (44), is given by an affine transformation of the entanglement distribution plotted in Fig. 4b,

$$4E_2(U_0^{(2)}|2,\mathbf{n}\rangle) = 9E_1(U_0^{\text{Eq. (41)}}|3/2,\mathbf{n}\rangle) - 5. \tag{65}$$

Thus, $E_2(U_0^{(2)}|2,\mathbf{n}\rangle)$ has icosahedral symmetry.

6. Average of e_{p} over the unitary orbit

We calculate the average of $e_{\mathrm{p}}(E_q, U)$ over the unitary operators $\mathrm{SU}(d)$, with $d = 2j+1$, and with respect to the normalized Haar measure ($\int \mathrm{d}\mu(U) = 1$)

$$\overline{e_{\mathrm{p}}(E_q,U)}^{\mathrm{SU}(d)} \equiv \int e_{\mathrm{p}}(E_q,U)\mathrm{d}\mu(U) = 1 - \frac{1}{2j+1-q}, \tag{66}$$

[2] Using the multipole expansion (A.2), each spin-1 operator has associated to it a spin-2 state. Specifically, the components $\rho_2(U)$ can be expressed as $|\rho_2(U)\rangle = \sum_{m=-2}^{2}\rho_{2m}(U)|2,m\rangle$. In particular, for $U = A \in \mathrm{SU}(3)$, where A is defined in Eq. (13), we obtain that $|\rho_2(A^{*2})\rangle \propto |\psi_A\rangle$ (see Eq. (59)). However, this proportionality does not extend to higher spins.

[3] The spin-3 states shown in Eq. (63) span a 3-dimensional 1-anticoherent subspace (see Ref. [42] for more details).

Table 2
Average of $e_{\mathrm{p}}(E_q, U)$ over the set of unitary gates SU($2j+1$) for several values of j and q. Additionally, we include the maximum possible value of e_{p} for $j = 1$ and 3/2, as well as the conjectured maximum values for $j = 2$ obtained from numerical searches.

j	q	$\overline{e_{\mathrm{p}}(E_q,U)}^{\mathrm{SU}(2j+1)}$	$\max_U e_{\mathrm{p}}(E_q,U)$
1	1	1/2	3/5
3/2	1	2/3	20/21
2	1	3/4	6889/7140
2	2	2/3	25/28

the details can be found in Appendix D. The last equation can be written in terms of the dimensions of the initial and the reduced Hilbert spaces, $\mathcal{H}^{(q/2)} \otimes \mathcal{H}^{(j-q/2)}$ and $\mathcal{H}^{(q/2)}$ respectively,

$$\overline{e_{\mathrm{p}}(E_q,U)}^{\mathrm{SU}(d)} = 1 - \frac{\dim(\mathcal{H}^{(q/2)})}{\dim(\mathcal{H}^{(q/2)} \otimes \mathcal{H}^{(j-q/2)})}. \tag{67}$$

We observe that, similar to the non-symmetric case [25], the average of e_{p} increases as the dimension of the initial (resp. reduced) Hilbert space increases (resp. decreases). However, this dependence differs from that of the non-symmetric case. To corroborate this, let us briefly review e_{p} in the non-symmetric case.

We start with a system of n qudits $\mathcal{H}_D^{\otimes n}$. Then, we calculate its average linear entanglement entropy after we trace out $n-q$ constituents, Q_q (see [25] for the formal definition), where the average here means over all the possible bipartitions $q|n-q$ over the n constituents. In particular, if the state is symmetric, $Q_q = E_q$. Now, the entangling power with respect to a unitary matrix $\mathbb{U} \in \mathrm{SU}(D^n)$, $e_{\mathrm{p}}(Q_q, \mathbb{U})$, is equal to

$$e_{\mathrm{p}}(Q_q,\mathbb{U}) = \int Q_q\Big(\mathbb{U}\big(|\psi_1\rangle \otimes |\psi_2\rangle \otimes \cdots \otimes |\psi_n\rangle\big)\Big)\mathrm{d}\mu(\psi_1)\ldots\mathrm{d}\mu(\psi_n), \tag{68}$$

where $\int \mathrm{d}\mu(\psi_k) = 1$. It turns out that its average over the unitary orbit SU(D^n) is equal to [25]

$$\overline{e_{\mathrm{p}}(Q_q,\mathbb{U})}^{\mathrm{SU}(D^n)} = 1 - \frac{\dim(\mathcal{H}_D^{\otimes q})+1}{\dim(\mathcal{H}_D^{\otimes n})+1}. \tag{69}$$

where $\dim(\mathcal{H}_D^{\otimes \alpha}) = D^\alpha$. We can observe a difference between the previous equation and Eq. (66), which is to be expected because we integrated over different sets of product states (see Eqs. (6) and (68)) and over different sets of unitary gates (see Eqs. (66) and (69)). We tabulate $\overline{e_{\mathrm{p}}(E_q,U)}$ for several values of j and q in Table 2. Similar discrepancies appear between the averages of the purity and linear entropy, over the symmetric sector and the entire Hilbert space of N qubits [43].

7. e_{p} and Schmidt numbers

The reformulation of e_{p} in Eq. (28) shows that the entangling power increases as the subspace associated with the image of $\mathcal{N} = \mathcal{P}_{2j}/(4j+1)$, $\mathrm{im}(\mathcal{N})$, is transformed to the orthogonal complement of $\mathcal{M}_q^{\perp}$. The Schmidt numbers of the states $|\psi\rangle \in \mathcal{H}^{(j)\otimes 2}$ are invariant under the action of $\mathcal{U}$. For instance, the states associated to coupled basis $|j,j,L,M\rangle$, or just $|L,M\rangle$ for short, have a Schmidt decomposition in terms of the decoupled basis $|j,m_1\rangle|j,m_2\rangle$. We write the explicit expressions for the states of $j = 1$ and 3/2 in Appendix E. In general, for a state $|\psi\rangle \in \mathrm{im}(\mathcal{P}_{2j})$ to be connected by a $\mathcal{U}$ transformation to a state $|\phi\rangle \in \mathrm{im}(\mathcal{P}_{2j}^{\perp})$, their Schmidt numbers have to be equal. We apply this idea to the search for the optimal unitary operators, for $j = 1$ and 3/2. In particular, this approach led us to the identification of U_0 for $j = 3/2$, *i.e.* , Eq. (41).

7.1. $N = 2$ ($j = 1$)

Eq. (36) implies that the unitary transformations $\mathcal{U} = U \otimes U$ that maximize e_{p} are those that transformed one state from $\mathrm{im}(\mathcal{P}_2)$ to $\mathrm{im}(\mathcal{P}_0)$. Here, $\mathcal{P}_0$ contains only one state given by (see Appendix E)

$$|0,0\rangle = \frac{1}{\sqrt{3}}\big(|1\rangle|-1\rangle - |0\rangle|0\rangle + |-1\rangle|1\rangle\big), \tag{70}$$

with Schmidt numbers $(1,1,1)/\sqrt{3}$. By direct inspection, we find that the state $|\Psi\rangle \in \mathrm{im}(\mathcal{P}_2)$ given by

$$|\Psi\rangle = \frac{1}{\sqrt{3}}\big(\sqrt{2}|2,1\rangle - |2,-2\rangle\big) = \frac{1}{\sqrt{3}}\big(|1\rangle|0\rangle - |-1\rangle|-1\rangle + |0\rangle|1\rangle\big) \tag{71}$$

can be transformed, via U_0' given in Eq. (17), to $U_0' \otimes U_0'|\Psi\rangle = |0,0\rangle \in \mathrm{im}(\mathcal{P}_0)$. Thus, U_0' maximizes e_{p}.

7.2. $N = 3$ ($j = 3/2$)

Similarly, Eq. (40) suggests that $\mathcal{U}$ must transform three vectors from $\mathrm{im}(\mathcal{P}_3)$ to $\mathrm{im}(\mathcal{P}_1)$ in order to optimize e_p. The $|1, M\rangle$ states have Schmidt numbers (see Appendix E)

$$\begin{aligned} &\frac{1}{\sqrt{10}}\left(\sqrt{3}, \sqrt{3}, 2, 0\right) \quad \text{for } M = \pm 1, \\ &\frac{1}{2\sqrt{5}}(3, 3, 1, 1) \quad \text{for } M = 0. \end{aligned} \tag{72}$$

We find that certain states in $\mathrm{im}(\mathcal{P}_3)$ have the same Schmidt numbers. Moreover, the $\mathcal{U}$ defined by Eq. (41) effects the desired transformation

$$\begin{aligned} \mathcal{U}\left(\sqrt{\frac{3}{5}}|3, \mp 2\rangle - \sqrt{\frac{2}{5}}|3, \pm 3\rangle\right) &= |1, \pm 1\rangle, \\ \mathcal{U}|3, 0\rangle &= |1, 0\rangle. \end{aligned} \tag{73}$$

8. Conclusions and perspectives

In this work we have studied the entangling power of unitary operators acting on symmetric states of $N = 2j$ qubits, which can be viewed as spin-j states. The main differences with respect to the general non-symmetric case is that the set of product states are reduced to the SC states (see Eq. (6)), and the set of unitary gates is reduced from $\mathrm{SU}(2^N)$ to $\mathrm{SU}(N+1)$ (See Section 6 for more details). e_p is reformulated as the inner product of two $(N+1)$-vectors (28). One vector, $\mathcal{M}_q$, depends on the linear entanglement entropy E_q, while the other vector, $\mathcal{N}$, is transformed by the unitary matrix U. The components of both vectors are SU(2)-invariant quantities, meaning that unitary transformations U, U', differing only by left or right rotations, $U' = R_1 U R_2$, preserve them. Following this approach, several results and derivations are obtained, also raising new questions, which we summarize below.

We study in detail e_p for states with a small number of qubits. Specifically, we identified the unitary gates that maximize $e_\mathrm{p}(E_1, U)$ for $N = 2$ and $N = 3$, given by Eqs. (17) and (41), respectively. Through numerical calculations, we also discovered two unitary gates, Eqs. (43)–(44), that are conjectured to maximize $e_\mathrm{p}(E_q, U)$ for $N = 4$ with $q = 1, 2$, respectively. These extremal unitaries possess highly symmetric entanglement distributions on the sphere (see Fig. 4) — note that a similar characteristic is observed for the extremal spin states that maximize entanglement measures [44–47]. Additionally, the hermitian matrices $\mathcal{D}_q(U)$ (48) of these extremal unitaries, associated with the entanglement distributions, display peculiar characteristics such as high point group symmetries and multiple degeneracies in their eigenspectra. Also notably, these extremal unitaries can be represented as linear combinations of at most two permutations matrices with complex entries. The e_p reduces to an expression that contains the sum of the eigenvalues of $\mathcal{D}_q$. We also point out that $e_\mathrm{p}(E_q, U) = e_\mathrm{p}(E_q, U^\dagger)$ holds true for $N = 2$ and 3, but fails, in general, for a higher number of qubits. This symmetry of e_p may be recast as time-reversal invariance, when U is generated by a hamiltonian, $U = e^{-itH}$.

We compute the average of $e_\mathrm{p}(E_q, U)$ over unitary gates $\mathrm{SU}(N+1)$ with respect to the Haar measure, Eq. (66), where we observe a difference with respect to the non-symmetric case Eq. (69). By sampling Haar-uniform random unitaries, we find that most of their associated invariant vectors cluster near the mean value (see Table 2). These observations indicate that random unitary gates exhibit a statistical distribution with a narrow spread around the mean value. Further work could be done to derive the explicit statistical distribution of $e_\mathrm{p}(E_q, U)$, as well as other variables such as the SU(2)-invariant components p_L (33).

The vectors introduced in our geometrical approach to the calculation of e_p have components associated to the subspace projectors $\mathcal{P}_L$. Thus, finding the maximum of e_p involves searching for the unitary gate that transforms a subspace into another. Additionally, unitary transformations do not alter the Schmidt decomposition of the states in $\mathcal{P}_L$, suggesting that an alternative approach to maximizing e_p is to examine the possible Schmidt decomposition for the states spanning $\mathrm{im}(\mathcal{P}_L)$. This approach proved useful in identifying the unitary gate that maximizes $e_\mathrm{p}(E_1, U)$ for $N = 3$. Another line of research, to be pursued in future work, is the calculation of the entangling power via the operator Schmidt decomposition, i.e., the intrinsic Schmidt decomposition of the unitary transformation U [16]. For the general (non-necessarily symmetric) case, the entangling power of U can be written in terms of its Schmidt numbers, the swap operator S, and the product US [16].

Lastly, we remark that, for spin-j pure states, the linear entanglement entropy E_q (3) coincides with the measure of anticoherence of order-q based on the purity (see Eq. (24) of Ref. [41]). Hence, the unitary gates with high (symmetric) entangling power correspond to those with high capacities to generate anticoherence in the SC states. Anticoherence for pure states is known to be a measure of non-classicality [48–51]. It is also known that anticoherent states are useful in quantum-enhanced metrology of rotations [42,46,52,53]. Other questions that broaden the scope of our work involve the semiclassical limit ($j \to \infty$) of our results. One could explore the general tendency of formulas such as Eq. (23) and the respective SU(2)-invariants, or consider a family of well-known symmetric unitary gates defined for any j and explore the behavior of their entangling power in the above limit.

In summary, we have examined in detail the concept of entangling power for unitary matrices acting on symmetric multiqubit states, introducing reformulations in terms of inner products between vectors associated to SU(2) invariants and transformation of subspaces of bipartite states among themselves. Additionally, the entanglement distribution of a unitary gate is associated with a linear combination of Husimi functions. These new perspectives could establish connections among quantities relevant for quantum information theory that initially appear unrelated, including those relevant to the non-symmetric case.

CRediT authorship contribution statement

Eduardo Serrano-Ensástiga: Writing – review & editing, Writing – original draft, Visualization, Validation, Supervision, Project administration, Methodology, Investigation, Formal analysis, Data curation, Conceptualization. **Diego Morachis Galindo:** Writing – review & editing, Investigation, Formal analysis. **Jesús A. Maytorena:** Writing – review & editing. **Chryssomalis Chryssomalakos:** Writing – review & editing, Methodology, Investigation, Conceptualization.

Declaration of competing interest

The authors declare that they have no known competing financial interests or personal relationships that could have appeared to influence the work reported in this paper.

Acknowledgments

ESE acknowledges support from the postdoctoral fellowship of the IPD-STEMA program of the University of Liège (Belgium). DMG acknowledges support from the F.R.S.-FNRS under the Excellence of Science (EOS) programme. CC acknowledges support from the UNAM-PAPIIT project IN112224. JAM and DMG acknowledge support from the UNAM-PAPIIT project IN111122 (México).

Appendix A. Master equation

Here, we derive Eq. (18). First, we introduce the basis of $\mathcal{HS}(\mathcal{H}^{(j)})$ defined by the *multipole operators* $\left\{T^{(j)}_{\sigma\mu}\right\}$, with $\sigma = 0,\dots,2j$ and $\mu = -\sigma,\dots,\sigma$ [38,54] and where we omit the superindex when there is no possible confusion. The $T_{\sigma\mu}$ operators can be written in terms of the Clebsch–Gordan coefficients $C^{jm}_{j_1m_1j_2m_2}$ [38] and they are orthonormal with respect to the HS scalar product

$$\mathrm{Tr}\left(T^{\dagger}_{\sigma_1\mu_1}T_{\sigma_2\mu_2}\right) = \delta_{\sigma_1\sigma_2}\delta_{\mu_1\mu_2}. \tag{A.1}$$

A density matrix $\rho \in \mathcal{HS}(\mathcal{H}^{(j)})$, representing a quantum state, can always be expanded in the $\{T_{\sigma\mu}\}$ basis

$$\rho = \sum_{\sigma=0}^{2j}\sum_{\mu=-\sigma}^{\sigma}\rho_{\sigma\mu}T_{\sigma\mu} = \sum_{\sigma=0}^{2j}\boldsymbol{\rho}_\sigma\cdot\mathbf{T}_\sigma, \tag{A.2}$$

where $\boldsymbol{\rho}_\sigma = \left(\rho_{\sigma\sigma},\dots,\rho_{\sigma-\sigma}\right)$ with $\rho_{\sigma\mu} = \mathrm{Tr}(\rho T^{\dagger}_{\sigma\mu})$, and $\mathbf{T}_\sigma = \left(T_{\sigma\sigma},\dots,T_{\sigma-\sigma}\right)$ is a vector of matrices. In particular, $T_{00} = (2j+1)^{-1/2}\mathbb{1}$, and then $\rho_{00} = (2j+1)^{-1/2}$ for any mixed state. In the picture of the spin-j states seen as $2j$-partite symmetric spin-1/2 systems, one can calculate the reduced density matrix $\rho_q = \mathrm{Tr}_{2j-q}\rho$, after tracing out $2j-q$ spins-1/2. Notably, the multipole expansion (A.2) of ρ_q has a simple expression in terms of the original state ρ [37,40]

$$\left(\rho_q\right)_{\sigma\mu} = \frac{q!}{(2j)!}\sqrt{\frac{(2j-\sigma)!(2j+\sigma+1)!}{(q-\sigma)!(q+\sigma+1)!}}\rho_{\sigma\mu}, \tag{A.3}$$

with $\sigma = 0,\dots,q$ and $\mu = -\sigma,\dots,\sigma$.

Now we calculate the entangling power (3) for a general spin-j system. First, we write the general expression of the SC states, transformed by U,

$$U|j,\mathbf{n}\rangle\langle j,\mathbf{n}|U^{\dagger} = \frac{1}{\sqrt{2j+1}}T^{(j)}_{00} + \sum_{\sigma=1}^{2j}\boldsymbol{\rho}_\sigma\cdot\mathbf{T}^{(j)}_\sigma, \tag{A.4}$$

with

$$\rho_{\sigma\mu} = \langle j,\mathbf{n}|U^{\dagger}T^{(j)\dagger}_{\sigma\mu}U|j,\mathbf{n}\rangle. \tag{A.5}$$

By tracing out the subsystem B, *i.e.* , $2j-q$ spin-1/2 constituents, we obtain

$$\begin{aligned}\rho_A =& \mathrm{Tr}_{2j-q}\left(U|j,\mathbf{n}\rangle\langle j,\mathbf{n}|U^{\dagger}\right)\\ =& \frac{1}{\sqrt{q+1}}T^{(q/2)}_{00} + \sum_{\sigma=1}^{q}\frac{q!}{(2j)!}\sqrt{\frac{(2j-\sigma)!(2j+\sigma+1)!}{(q-\sigma)!(q+\sigma+1)!}}\boldsymbol{\rho}_\sigma\cdot\mathbf{T}^{(q/2)}_\sigma,\end{aligned} \tag{A.6}$$

where we use Eq. (A.3). We then get that

$$\begin{aligned}E_q(U|j,\mathbf{n}\rangle) =& 1 - \frac{(q+1)(q!)^2}{q(2j)!^2}\sum_{\sigma=1}^{q}\frac{(2j-\sigma)!(2j+\sigma+1)!}{(q-\sigma)!(q+\sigma+1)!}\left|\boldsymbol{\rho}_\sigma\right|^2,\\ =& 1 - \langle j,\mathbf{n}|\otimes\langle j,\mathbf{n}|\mathcal{U}^{\dagger}\mathcal{M}_q\mathcal{U}|j,\mathbf{n}\rangle\otimes|j,\mathbf{n}\rangle\end{aligned} \tag{A.7}$$

where $\mathcal{U} = U\otimes U$ as defined in the main text,

$$\mathcal{T}_\sigma = \sum_{\mu=-\sigma}^{\sigma}T_{\sigma\mu}\otimes T^{\dagger}_{\sigma\mu} \tag{A.8}$$

Table A.3
Vectors of SU(2) invariants of the operators $\mathcal{N}$ and $\mathcal{M}_q$ (A.9) in the $\mathcal{T}_\sigma$ basis for the spin values $j = 1, 3/2, 2, 5/2$ and $q = 1, \dots, \lfloor j \rfloor$. The vector $\overrightarrow{\mathcal{M}_q}$ has q non-zero entries.

j	$\overrightarrow{\mathcal{N}}$ in $\mathcal{T}_\sigma$ basis	$\overrightarrow{\mathcal{M}_q}$ in $\mathcal{T}_\sigma$ basis
1	$\left(\frac{1}{3}, \frac{1}{2\sqrt{3}}, \frac{1}{6\sqrt{5}}\right)$	$\left(0, 2\sqrt{3}, 0\right)$
3/2	$\left(\frac{1}{4}, \frac{3\sqrt{3}}{20}, \frac{1}{4\sqrt{5}}, \frac{1}{20\sqrt{7}}\right)$	$\left(0, \frac{20}{3\sqrt{3}}, 0, 0\right)$
2	$\left(\frac{1}{5}, 0, \frac{2}{5\sqrt{3}}, \frac{2}{7\sqrt{5}}, \frac{1}{10\sqrt{7}}, \frac{1}{210}\right)$	$\left(0, \frac{5\sqrt{3}}{2}, 0, 0, 0\right)$ $\left(0, \frac{15\sqrt{3}}{8}, \frac{7\sqrt{5}}{8}, 0, 0\right)$
5/2	$\left(\frac{1}{6}, 0, \frac{5}{14\sqrt{3}}, \frac{5\sqrt{5}}{84}, \frac{5}{36\sqrt{7}}, \frac{1}{84}, \frac{1}{252\sqrt{11}}\right)$	$\left(0, \frac{14\sqrt{3}}{5}, 0, 0, 0, 0\right)$ $\left(0, \frac{21\sqrt{3}}{10}, \frac{21}{5\sqrt{5}}, 0, 0, 0\right)$

and

$$\mathcal{M}_q = \frac{(q+1)(q!)^2}{q(2j)!^2} \sum_{\sigma=1}^{q} \frac{(2j-\sigma)!(2j+\sigma+1)!}{(q-\sigma)!(q+\sigma+1)!} \mathcal{T}_\sigma = \frac{q+1}{q} \sum_{\sigma=1}^{q} \frac{\begin{Bmatrix} q/2 & q/2 & q \\ q/2 & q/2 & \sigma \end{Bmatrix}}{\begin{Bmatrix} j & j & 2j \\ j & j & \sigma \end{Bmatrix}} \mathcal{T}_\sigma \,. \tag{A.9}$$

The $\mathcal{T}_\sigma$'s can be written as a linear combination of the $\mathcal{P}_L$ operators (see Identity 1 of Appendix C)

$$\mathcal{T}_\sigma = (2\sigma+1) \sum_{L=0}^{2j} (-1)^{2j+L} \begin{Bmatrix} j & j & L \\ j & j & \sigma \end{Bmatrix} \mathcal{P}_L. \tag{A.10}$$

This result gives the expression (19) of $\mathcal{M}_q$. Lastly, we use that $|j, \mathbf{n}\rangle \otimes |j, \mathbf{n}\rangle = |2j, \mathbf{n}\rangle$ to obtain Eq. (18).

Appendix B. The T operator basis

Identity 1 of Appendix C lets us write e_{p} (18) as an inner product of vectors of SU(2) invariants associated to the $\mathcal{T}_\sigma$ operators. The operator $\mathcal{M}_q$ is written in Eq. (A.9), while $\mathcal{N}$ is expanded as

$$\mathcal{N} = \sum_{L=0}^{2j} \begin{Bmatrix} j & j & 2j \\ j & j & L \end{Bmatrix} \mathcal{T}_L. \tag{B.1}$$

The $\mathcal{T}_\sigma$ operators are hermitian, orthogonal $\mathrm{Tr}(\mathcal{T}_\sigma \mathcal{T}_{\sigma'}) = (2\sigma+1)\delta_{\sigma\sigma'}$, and invariant under diagonal SU(2) transformations in the double-copy space $\mathcal{H}^{(j)\otimes 2}$. Thus, similarly as in Section 3, we associate to every operator $V \in \mathcal{HS}(\mathcal{H}^{(j)\otimes 2})$ a $(2j+1)$-vector of SU(2) invariants

$$\overrightarrow{V}^{\mathcal{T}} = \left(\mathrm{Tr}\left(V\tilde{\mathcal{T}}_0\right), \dots, \mathrm{Tr}\left(V\tilde{\mathcal{T}}_\sigma\right), \dots, \mathrm{Tr}\left(V\tilde{\mathcal{T}}_{2j}\right)\right), \tag{B.2}$$

with $\tilde{\mathcal{T}}_\sigma = \mathcal{T}_\sigma/\sqrt{2\sigma+1}$, and where the superscript denotes that the vector is written in the $\mathcal{T}$ basis. We follow the same procedure as in Section 3 to obtain a similar reformulation of e_{p} as an inner product of two vectors given in Eqs. (25)–(28) but now expressed in the $\mathcal{T}$ basis. We also have that each vector, now written in the $\mathcal{T}$ basis, lies in a hyperplane, even after the action of U,

$$\sum_{\sigma=0}^{2j} \left(\widehat{\mathcal{U}}\overrightarrow{\mathcal{N}}\right)_\sigma^{\mathcal{T}} = \sum_{\sigma=0}^{2j} \mathrm{Tr}\left(\mathcal{U}\mathcal{N}\mathcal{U}^\dagger \mathcal{T}_\sigma\right) = 1\,, \qquad \sum_{\sigma=0}^{2j} \left(\widehat{\mathcal{U}}\overrightarrow{\mathcal{M}_q}\right)_\sigma^{\mathcal{T}} = \frac{2(j+1)(2j+1)}{(2j-q+1)}. \tag{B.3}$$

We prove these results in Identity 3 of Appendix C. Since $\mathcal{T}_0$ is proportional to the identity, $\left(\widehat{\mathcal{U}}\overrightarrow{V}\right)_0^{\mathcal{T}} = \left(\overrightarrow{V}\right)_0^{\mathcal{T}}$. In particular $\left(\overrightarrow{\mathcal{N}}\right)_0^{\mathcal{T}} = 1/(2j+1)$ and $\left(\overrightarrow{\mathcal{M}_q}\right)_0^{\mathcal{T}} = 0$. We write $\mathcal{N}$ and $\mathcal{M}_q$ for $j = 1, 3/2, 2$ and $5/2$ in the $\mathcal{T}$ basis in Table A.3. The properties of the 6j-symbols show that the components of $\overrightarrow{\mathcal{N}}$ and $\overrightarrow{\mathcal{M}_q}$ are always positive in the $\mathcal{T}$ basis [38]. However, the disadvantage of the $\mathcal{T}$ basis is that a $\mathcal{U}$ transformation combines all the $\mathcal{T}$ components, not only half of them as in the $\mathcal{P}$ basis.

Appendix C. Useful identities

Here we prove several identities used throughout the paper.

Identity 1. *The operators $\mathcal{T}_\sigma$ and $\mathcal{P}_L$ are related by an invertible linear transformation,*

$$\mathcal{T}_\sigma = (2\sigma+1) \sum_{L=0}^{2j} (-1)^{2j+L} \begin{Bmatrix} j & j & L \\ j & j & \sigma \end{Bmatrix} \mathcal{P}_L, \qquad \mathcal{P}_L = (-1)^{2j+L}(2L+1) \sum_{\sigma=0}^{2j} \begin{Bmatrix} j & j & \sigma \\ j & j & L \end{Bmatrix} \mathcal{T}_\sigma. \tag{C.1}$$

Proof.

$$
\begin{aligned}
\mathcal{T}_\sigma &= \sum_{\mu=-\sigma}^{\sigma} T_{\sigma\mu}\otimes T^\dagger_{\sigma\mu} \\
&= \left(\frac{2\sigma+1}{2j+1}\right)\sum_{\mu}\sum_{\substack{m,m'\\ n,n'}} C^{jm}_{jm',\sigma\mu}C^{jn}_{jn',\sigma\mu}|j,m\rangle\langle j,m'|\otimes|j,n'\rangle\langle j,n| \\
&= \left(\frac{2\sigma+1}{2j+1}\right)\sum_{\mu}\sum_{\substack{m,m'\\ n,n'}}\sum_{\substack{L_1,M_1\\ L_2,M_2}} C^{jm}_{jm',\sigma\mu}C^{jn}_{jn',\sigma\mu}C^{L_1M_1}_{jm,jn'}C^{L_2M_2}_{jm',jn}|j,j,L_1,M_1\rangle\langle j,j,L_2,M_2| \\
&= \left(\frac{2\sigma+1}{2j+1}\right)(-1)^{\sigma}\sum_{\substack{L_1,M_1\\ L_2,M_2}}\sum_{M}\sum_{\substack{m,m'\\ n,n'}} C^{L_1M_1}_{jm,jn'}C^{jm}_{jm',\sigma\mu}C^{L_2M_2}_{jm',jn}C^{jn}_{\sigma\mu,jn'}|j,j,L_1,M_1\rangle\langle j,j,L_2,M_2| \\
&= (2\sigma+1)\sum_{L_1,M_1}(-1)^{2j+L_1}\begin{Bmatrix} j & j & L_1\\ j & j & \sigma\end{Bmatrix}|L_1,M_1\rangle_C\langle L_1,M_1|_C \\
&= (2\sigma+1)\sum_{L=0}^{2j}(-1)^{2j+L}\begin{Bmatrix} j & j & L\\ j & j & \sigma\end{Bmatrix}\mathcal{P}_L,
\end{aligned}
\tag{C.2}
$$

where we use the decoupled and coupled bases of the angular momentum (8) and the definition of the 6j symbol (see p. 291, Eq. (8) of Ref. [38]). Lastly, we invert the previous equation with the orthogonality of the 6j symbols (See page 291 or Ref. [38] for the general formula)

$$
(2\sigma+1)\sum_{L=0}^{2j}(2L+1)\begin{Bmatrix} j & j & L\\ j & j & \sigma\end{Bmatrix}\begin{Bmatrix} j & j & L\\ j & j & \sigma'\end{Bmatrix} = \delta_{\sigma\sigma'},
\tag{C.3}
$$

to write $\mathcal{P}_L$ in terms of the operators $\mathcal{T}_\sigma$. □

Identity 2. *For any unitary transformation $\mathcal{U} = U\otimes U$ and operator $V = \sum_{K=0}^{2j} v_K\mathcal{P}_K$, it holds that*

$$
\sum_{\substack{L=0\\ 2j\equiv L+\delta \pmod 2}}^{2j} Tr\left(\mathcal{U}V\mathcal{U}^\dagger\mathcal{P}_L\right) = \sum_{\substack{L=0\\ 2j\equiv L+\delta \pmod 2}}^{2j} Tr\left(V\mathcal{P}_L\right),
\tag{C.4}
$$

for $\delta = 0$ and 1. In particular,

$$
\sum_{\substack{L=0\\ K\equiv L \pmod 2}}^{2j} Tr\left(\mathcal{U}\mathcal{P}_L\mathcal{U}^\dagger\mathcal{P}_K\right) = 2K+1, \qquad \sum_{\substack{L=0\\ 2j\equiv L \pmod 2}}^{2j} Tr\left(\mathcal{U}\mathcal{P}_L\mathcal{U}^\dagger\mathcal{M}_q\right) = \frac{(j+1)(2j+1)}{2j+1-q}.
\tag{C.5}
$$

Proof. By resolution of the unity of the $\mathcal{P}_L$ operators, we have that

$$
\sum_{L=0}^{2j}\mathrm{Tr}\left(\mathcal{U}\mathcal{P}_L\mathcal{U}^\dagger\mathcal{P}_K\right) = \mathrm{Tr}\left(\mathcal{P}_K\right) = 2K+1.
\tag{C.6}
$$

Now, the unitary transformations $\mathcal{U} = U\otimes U$ preserve the orthogonality between the projectors of different parity

$$
\mathrm{Tr}(\mathcal{U}\mathcal{P}_L\mathcal{U}^\dagger\mathcal{P}_K) = 0, \quad \text{for } L\equiv K+1 \pmod 2,
\tag{C.7}
$$

because they preserve the permutation exchange of the states $|\Psi\rangle\in\mathcal{H}^{(j)\otimes 2}$. Thus, any operator $V = \sum_{K=0}^{2j} v_K\mathcal{P}_K$ can be split in the components with K odd and even, and these components do not mix after a transformation by $\mathcal{U}$. This proves (C.4). In particular,

$$
\sum_{L=0}^{2j}\mathrm{Tr}\left(\mathcal{U}\mathcal{P}_L\mathcal{U}^\dagger\mathcal{P}_K\right) = \sum_{\substack{L=0\\ K\equiv L \pmod 2}}^{2j}\mathrm{Tr}\left(\mathcal{U}\mathcal{P}_L\mathcal{U}^\dagger\mathcal{P}_K\right) = \mathrm{Tr}\left(\mathcal{P}_K\right) = 2K+1.
\tag{C.8}
$$

For $\mathcal{M}_q$, we have that

$$
\sum_{\substack{L=0\\ 2j\equiv L+\delta \pmod 2}}^{2j}\mathrm{Tr}\left(\mathcal{U}\mathcal{M}_q\mathcal{U}^\dagger\mathcal{P}_L\right) = \frac{1}{2}\sum_{L=0}^{2j}\left[1+(-1)^{2j+L+\delta}\right]\mathrm{Tr}\left(\mathcal{M}_q\mathcal{P}_L\right) = (-1)^\delta\frac{(j+1)(2j+1)}{2j+1-q},
\tag{C.9}
$$

where we use identities of the 6j symbols [38]. □

Identity 3. *Any hermitian operator $V = \sum_{\sigma=0}^{2j} v_\sigma\mathcal{T}_\sigma$ satisfies*

$$
\sum_{\sigma=0}^{2j} Tr\left(\mathcal{U}V\mathcal{U}^\dagger\mathcal{T}_\sigma\right) = \sum_{\sigma=0}^{2j} Tr\left(V\mathcal{T}_\sigma\right),
\tag{C.10}
$$

where $\mathcal{U} = U \otimes U$ and U a unitary operator. In particular,

$$\sum_{\sigma=0}^{2j} Tr\left(\mathcal{M}_q \mathcal{T}_\sigma\right) = \frac{2(j+1)(2j+1)}{(2j-q+1)}, \qquad \sum_{\sigma=0}^{2j} Tr\left(\mathcal{N} \mathcal{T}_\sigma\right) = \frac{2j}{2j+1}. \tag{C.11}$$

Proof. The following calculation will prove convenient later on,

$$\begin{aligned}\sum_{\sigma=0}^{2j} \mathcal{T}_\sigma &= \sum_{\sigma=0}^{2j} \sum_{\mu=-\sigma}^{\sigma} \sum_{\substack{m_1,m_2\\ n_1,n_2}} (-1)^{2j-m_2-n_2} C^{\sigma\mu}_{jm_1 j-m_2} C^{\sigma\mu}_{jn_1 j-n_2} |j,m_1,j,n_2\rangle\langle j,m_2,j,n_1| \\ &= \sum_{\substack{m_1,m_2\\ n_1,n_2}} (-1)^{2j-m_2-n_2} \delta_{m_1,n_1}\delta_{m_2 n_2} |j,m_1,j,n_2\rangle\langle j,m_2,j,n_1| \\ &= \sum_{m_1,m_2} |j,m_1,j,m_2\rangle\langle j,m_2,j,m_1|\end{aligned} \tag{C.12}$$

where we use that $2(j-m)$ is always an even integer number. Now, let us prove the result for the $\mathcal{T}_\sigma$ operators

$$\sum_{\sigma=0}^{2j} \mathrm{Tr}\left(\mathcal{U}^\dagger \mathcal{T}_\tau \mathcal{U} \mathcal{T}_\sigma\right) = \sum_{\nu=-\tau}^{\tau} \sum_{m_1,m_2} \langle j,m_2|U^\dagger T_{\tau\nu} U|j,m_1\rangle\langle j,m_1|U^\dagger T^\dagger_{\tau\nu} U|j,m_2\rangle = 2\tau+1 = \sum_{\sigma=0}^{2j} \mathrm{Tr}\left(\mathcal{T}_\tau \mathcal{T}_\sigma\right), \tag{C.13}$$

The first equality will be valid for any V by linearity. In particular, we get for $V = \mathcal{N}$ that

$$\sum_{\sigma=0}^{2j} \mathrm{Tr}\left(\mathcal{N}\mathcal{T}_\sigma\right) = \sum_{\sigma=0}^{2j}\sum_{L=1}^{2j} \begin{Bmatrix} j & j & 2j \\ j & j & L \end{Bmatrix} \mathrm{Tr}\left(\mathcal{T}_L \mathcal{T}_\sigma\right) = \sum_{L=1}^{2j} (2L+1) \begin{Bmatrix} j & j & 2j \\ j & j & L \end{Bmatrix} = \frac{2j}{2j+1}, \tag{C.14}$$

where we use the following identities of the 6j symbol [38]

$$\sum_{L=0}^{2j} (2L+1) \begin{Bmatrix} j & j & 2j \\ j & j & L \end{Bmatrix} = 1, \qquad \begin{Bmatrix} j & j & 2j \\ j & j & 0 \end{Bmatrix} = \frac{1}{2j+1}. \tag{C.15}$$

Similarly,

$$\sum_{\sigma=0}^{2j} \mathrm{Tr}\left(\mathcal{M}_q \mathcal{T}_\sigma\right) = \frac{q+1}{q} \sum_{\tau=1}^{q} (2\tau+1) \frac{\begin{Bmatrix} q/2 & q/2 & q \\ q/2 & q/2 & \tau \end{Bmatrix}}{\begin{Bmatrix} j & j & 2j \\ j & j & \tau \end{Bmatrix}} = \frac{2(j+1)(2j+1)}{2j+1-q}. \qquad \square \tag{C.16}$$

Appendix D. Proof of Eq. (66)

We start with the following identity regarding the integration over the SU(d) unitary matrices and where A is a $d^2 \times d^2$ matrix (see **Proposition 3.9** in [55])

$$\int \mathcal{U} A \mathcal{U}^\dagger \mathrm{d}\mu(U) = \left[\frac{\mathrm{Tr}(A)}{d^2-1} - \frac{\mathrm{Tr}(AF)}{d(d^2-1)}\right] \mathbb{1}_{d^2} - \left[\frac{\mathrm{Tr}(A)}{d(d^2-1)} - \frac{\mathrm{Tr}(AF)}{d^2-1}\right] F \tag{D.1}$$

where $F|\psi_1\rangle|\psi_2\rangle = |\psi_2\rangle|\psi_1\rangle$ is the swap operator. In particular $F\mathcal{P}_L = \mathcal{P}_L F = (-1)^{2j-L}\mathcal{P}_L$. Thus,

$$\int e_{\mathrm{p}}(E_q,U)\mathrm{d}\mu(U) = 1 - \mathrm{Tr}\left(\left[\int \mathcal{U}\mathcal{N}\mathcal{U}^\dagger \mathrm{d}\mu(U)\right]\mathcal{M}_q\right) = 1 - \frac{1}{d(d+1)}\left[\mathrm{Tr}\left(\mathcal{M}_q\right) + \mathrm{Tr}\left(F\mathcal{M}_q\right)\right]. \tag{D.2}$$

We add the resolution of the unity $\mathbb{1}_{d^2} = \sum_{L=0}^{2j} \mathcal{P}_L$ to use Eq. (C.9) in the last equation

$$\int e_{\mathrm{p}}(E_q,U)\mathrm{d}\mu(U) = 1 - \frac{2(j+1)(2j+1)}{d(d+1)(2j+1-q)} = \frac{2j-q}{2j+1-q}. \tag{D.3}$$

Appendix E. Spin states in the coupled and decoupled bases

Here, we write the coupled basis $|L,M\rangle \equiv |j_1,j_2,L,M\rangle$ in terms of the decoupled basis $|m_1\rangle|m_2\rangle \equiv |j_1,m_1\rangle|j_2 m_2\rangle$. For $j=1$, we have

$$\begin{aligned}|2,\pm2\rangle &= |\pm1\rangle|\pm1\rangle, \\ |2,\pm1\rangle &= \frac{1}{\sqrt{2}}\left(|\pm1\rangle|0\rangle + |0\rangle|\pm1\rangle\right), \\ |2,0\rangle &= \frac{1}{\sqrt{6}}\left(|1\rangle|-1\rangle + 2|0\rangle|0\rangle + |-1\rangle|1\rangle\right), \\ |0,0\rangle &= \frac{1}{\sqrt{3}}\left(|1\rangle|-1\rangle - |0\rangle|0\rangle + |-1\rangle|1\rangle\right),\end{aligned} \tag{E.1}$$

And for $j = 3/2$, it reads

$$
\begin{aligned}
|3,\pm3\rangle &= \left|\pm\frac{3}{2}\right\rangle\left|\pm\frac{3}{2}\right\rangle,\\
|3,\pm2\rangle &= \frac{1}{\sqrt{2}}\left(\left|\pm\frac{3}{2}\right\rangle\left|\pm\frac{1}{2}\right\rangle + \left|\pm\frac{1}{2}\right\rangle\left|\pm\frac{3}{2}\right\rangle\right),\\
|3,\pm1\rangle &= \frac{1}{\sqrt{5}}\left(\left|\pm\frac{3}{2}\right\rangle\left|\mp\frac{1}{2}\right\rangle + \left|\mp\frac{1}{2}\right\rangle\left|\pm\frac{3}{2}\right\rangle + \sqrt{3}\left|\pm\frac{1}{2}\right\rangle\left|\pm\frac{1}{2}\right\rangle\right),\\
|3,0\rangle &= \frac{1}{2\sqrt{5}}\left(\left|\frac{3}{2}\right\rangle\left|-\frac{3}{2}\right\rangle + \left|-\frac{3}{2}\right\rangle\left|\frac{3}{2}\right\rangle + 3\left|\frac{1}{2}\right\rangle\left|-\frac{1}{2}\right\rangle + 3\left|-\frac{1}{2}\right\rangle\left|\frac{1}{2}\right\rangle\right),
\end{aligned}
\tag{E.2}
$$

$$
\begin{aligned}
|1,\pm1\rangle &= \frac{1}{\sqrt{10}}\left(\sqrt{3}\left|\pm\frac{3}{2}\right\rangle\left|\mp\frac{1}{2}\right\rangle + \sqrt{3}\left|\mp\frac{1}{2}\right\rangle\left|\pm\frac{3}{2}\right\rangle - 2\left|\pm\frac{1}{2}\right\rangle\left|\pm\frac{1}{2}\right\rangle\right),\\
|1,0\rangle &= \frac{1}{2\sqrt{5}}\left(3\left|\frac{3}{2}\right\rangle\left|-\frac{3}{2}\right\rangle + 3\left|-\frac{3}{2}\right\rangle\left|\frac{3}{2}\right\rangle - \left|\frac{1}{2}\right\rangle\left|-\frac{1}{2}\right\rangle - \left|-\frac{1}{2}\right\rangle\left|\frac{1}{2}\right\rangle\right),
\end{aligned}
\tag{E.3}
$$

Data availability

Data will be made available on request.

References

[1] R. Horodecki, P. Horodecki, M. Horodecki, K. Horodecki, Quantum entanglement, Rev. Modern Phys. 81 (2009) 865–942, http://dx.doi.org/10.1103/RevModPhys.81.865.

[2] M.A. Nielsen, I.L. Chuang, Quantum Computation and Quantum Information: 10th Anniversary Edition, Tenth, Cambridge University Press, New York, NY, USA, 2011.

[3] I. Bengtsson, K. Życzkowski, Geometry of Quantum States (2nd Ed.), Cambridge University Press, 2017.

[4] W. Dür, G. Vidal, J.I. Cirac, N. Linden, S. Popescu, Entanglement capabilities of nonlocal Hamiltonians, Phys. Rev. Lett. 87 (2001) 137901, http://dx.doi.org/10.1103/PhysRevLett.87.137901.

[5] M.M. Wolf, J. Eisert, M.B. Plenio, Entangling power of passive optical elements, Phys. Rev. Lett. 90 (2003) 047904, http://dx.doi.org/10.1103/PhysRevLett.90.047904.

[6] H.-N. Xiong, X.-M. Lu, X. Wang, Partial entangling power for the Jaynes–Cummings model, J. Phys. B: At. Mol. Opt. Phys. 45 (1) (2011) 015501, http://dx.doi.org/10.1088/0953-4075/45/1/015501.

[7] B. Kraus, J.I. Cirac, Optimal creation of entanglement using a two-qubit gate, Phys. Rev. A 63 (2001) 062309, http://dx.doi.org/10.1103/PhysRevA.63.062309.

[8] J. Zhang, J. Vala, S. Sastry, K.B. Whaley, Geometric theory of nonlocal two-qubit operations, Phys. Rev. A 67 (2003) 042313, http://dx.doi.org/10.1103/PhysRevA.67.042313.

[9] T. Kalsi, A. Romito, H. Schomerus, Three-fold way of entanglement dynamics in monitored quantum circuits, J. Phys. A 55 (26) (2022) 264009, http://dx.doi.org/10.1088/1751-8121/ac71e8.

[10] H.L. Tang, K. Connelly, A. Warren, F. Zhuang, S.E. Economou, E. Barnes, Designing globally time-optimal entangling gates using geometric space curves, Phys. Rev. Appl. 19 (2023) 044094, http://dx.doi.org/10.1103/PhysRevApplied.19.044094.

[11] F. Caruso, A.W. Chin, A. Datta, S.F. Huelga, M.B. Plenio, Entanglement and entangling power of the dynamics in light-harvesting complexes, Phys. Rev. A 81 (2010) 062346, http://dx.doi.org/10.1103/PhysRevA.81.062346.

[12] P. Zanardi, C. Zalka, L. Faoro, Entangling power of quantum evolutions, Phys. Rev. A 62 (2000) 030301, http://dx.doi.org/10.1103/PhysRevA.62.030301.

[13] M.A. Nielsen, C.M. Dawson, J.L. Dodd, A. Gilchrist, D. Mortimer, T.J. Osborne, M.J. Bremner, A.W. Harrow, A. Hines, Quantum dynamics as a physical resource, Phys. Rev. A 67 (2003) 052301, http://dx.doi.org/10.1103/PhysRevA.67.052301.

[14] B. Jonnadula, P. Mandayam, K. Życzkowski, A. Lakshminarayan, Impact of local dynamics on entangling power, Phys. Rev. A 95 (2017) 040302, http://dx.doi.org/10.1103/PhysRevA.95.040302.

[15] L. Clarisse, S. Ghosh, S. Severini, A. Sudbery, The disentangling power of unitaries, Phys. Lett. A 365 (5) (2007) 400–402, http://dx.doi.org/10.1016/j.physleta.2007.02.001.

[16] P. Zanardi, Entanglement of quantum evolutions, Phys. Rev. A 63 (2001) 040304, http://dx.doi.org/10.1103/PhysRevA.63.040304.

[17] A.T. Rezakhani, Characterization of two-qubit perfect entanglers, Phys. Rev. A 70 (2004) 052313, http://dx.doi.org/10.1103/PhysRevA.70.052313.

[18] S. Balakrishnan, R. Sankaranarayanan, Characterizing the geometrical edges of nonlocal two-qubit gates, Phys. Rev. A 79 (2009) 052339, http://dx.doi.org/10.1103/PhysRevA.79.052339.

[19] Y. Shen, L. Chen, Entangling power of two-qubit unitary operations, J. Phys. A 51 (39) (2018) 395303, http://dx.doi.org/10.1088/1751-8121/aad7cb.

[20] X. Wang, B.C. Sanders, D.W. Berry, Entangling power and operator entanglement in qudit systems, Phys. Rev. A 67 (2003) 042323, http://dx.doi.org/10.1103/PhysRevA.67.042323.

[21] Y. Yang, X. Wang, Z. Sun, Entangling power of a two-qudit geometric phase gate, Phys. Lett. A 372 (24) (2008) 4369–4372, http://dx.doi.org/10.1016/j.physleta.2008.04.023.

[22] M. Musz, M. Kuś, K. Życzkowski, Unitary quantum gates, perfect entanglers, and unistochastic maps, Phys. Rev. A 87 (2013) 022111, http://dx.doi.org/10.1103/PhysRevA.87.022111.

[23] J. Chen, Z. Ji, D.W. Kribs, B. Zeng, F. Zhang, Minimum entangling power is close to its maximum, J. Phys. A 52 (21) (2019) 215302, http://dx.doi.org/10.1088/1751-8121/ab15e3.

[24] F.-Z. Kong, J.-L. Zhao, Generating a maximally entangled state via a pure global noise environment, Laser Phys. Lett. 21 (5) (2024) 055206, http://dx.doi.org/10.1088/1612-202X/ad3627.

[25] A.J. Scott, Multipartite entanglement, quantum-error-correcting codes, and entangling power of quantum evolutions, Phys. Rev. A 69 (2004) 052330, http://dx.doi.org/10.1103/PhysRevA.69.052330.

[26] T. Linowski, G. Rajchel-Mieldzioć, K. Życzkowski, Entangling power of multipartite unitary gates, J. Phys. A 53 (12) (2020) 125303, http://dx.doi.org/10.1088/1751-8121/ab749a.
[27] X. Wang, P. Zanardi, Quantum entanglement of unitary operators on bipartite systems, Phys. Rev. A 66 (2002) 044303, http://dx.doi.org/10.1103/PhysRevA.66.044303.
[28] Y. Makhlin, Nonlocal properties of two-qubit gates and mixed states, and the optimization of quantum computations, Quantum Inf. Process. 1 (2002) 243–252, http://dx.doi.org/10.1023/A:1022144002391.
[29] S. Balakrishnan, R. Sankaranarayanan, Entangling power and local invariants of two-qubit gates, Phys. Rev. A 82 (2010) 034301, http://dx.doi.org/10.1103/PhysRevA.82.034301.
[30] S. Singh, I. Nechita, Diagonal unitary and orthogonal symmetries in quantum theory: Ii. evolution operators, J. Phys. A 55 (25) (2022) 255302, http://dx.doi.org/10.1088/1751-8121/ac7017.
[31] A.J. Scott, C.M. Caves, Entangling power of the quantum baker's map, J. Phys. A: Math. Gen. 36 (36) (2003) 9553, http://dx.doi.org/10.1088/0305-4470/36/36/308.
[32] R. Pal, A. Lakshminarayan, Entangling power of time-evolution operators in integrable and nonintegrable many-body systems, Phys. Rev. B 98 (2018) 174304, http://dx.doi.org/10.1103/PhysRevB.98.174304.
[33] S. Aravinda, S.A. Rather, A. Lakshminarayan, From dual-unitary to quantum Bernoulli circuits: Role of the entangling power in constructing a quantum ergodic hierarchy, Phys. Rev. Res. 3 (2021) 043034, http://dx.doi.org/10.1103/PhysRevResearch.3.043034.
[34] C. Chryssomalakos, E. Guzmán-González, E. Serrano-Ensástiga, Geometry of spin coherent states, J. Phys. A: Math. Theor. 51 (16) (2018) 165202, http://dx.doi.org/10.1088/1751-8121/aab349.
[35] D. Morachis Galindo, J.A. Maytorena, Entangling power of symmetric two-qubit quantum gates and three-level operations, Phys. Rev. A 105 (2022) 012601, http://dx.doi.org/10.1103/PhysRevA.105.012601.
[36] M. Byrd, Differential geometry on SU(3) with applications to three state systems, J. Math. Phys. 39 (11) (1998) 6125–6136, http://dx.doi.org/10.1063/1.532618.
[37] J. Denis, J. Martin, Extreme depolarization for any spin, Phys. Rev. Res. 4 (2022) 013178, http://dx.doi.org/10.1103/PhysRevResearch.4.013178.
[38] D. Varshalovich, A. Moskalev, V. Khersonskii, Quantum Theory of Angular Momentum, World Scientific, 1988.
[39] G.S. Agarwal, Relation between atomic coherent-state representation, state multipoles, and generalized phase-space distributions, Phys. Rev. A 24 (1981) 2889–2896, http://dx.doi.org/10.1103/PhysRevA.24.2889.
[40] E. Serrano-Ensástiga, D. Braun, Majorana representation for mixed states, Phys. Rev. A 101 (2) (2020) 022332, http://dx.doi.org/10.1103/PhysRevA.101.022332.
[41] D. Baguette, J. Martin, Anticoherence measures for pure spin states, Phys. Rev. A 96 (2017) 032304, http://dx.doi.org/10.1103/PhysRevA.96.032304.
[42] E. Serrano-Ensástiga, C. Chryssomalakos, J. Martin, Quantum metrology of rotations with mixed spin states, Phys. Rev. A 111 (2025) 022435, http://dx.doi.org/10.1103/PhysRevA.111.022435.
[43] A. Seshadri, V. Madhok, A. Lakshminarayan, Tripartite mutual information, entanglement, and scrambling in permutation symmetric systems with an application to quantum chaos, Phys. Rev. E 98 (2018) 052205, http://dx.doi.org/10.1103/PhysRevE.98.052205.
[44] J. Martin, O. Giraud, P.A. Braun, D. Braun, T. Bastin, Multiqubit symmetric states with high geometric entanglement, Phys. Rev. A 81 (2010) 062347, http://dx.doi.org/10.1103/PhysRevA.81.062347.
[45] O. Giraud, P. Braun, D. Braun, Quantifying quantumness and the quest for queens of quantum, New J. Phys. 12 (6) (2010) 063005, http://dx.doi.org/10.1088/1367-2630/12/6/063005.
[46] C. Chryssomalakos, L. Hanotel, E. Guzmán-González, D. Braun, E. Serrano-Ensástiga, K. Życzkowski, Symmetric multiqudit states: Stars, entanglement, and rotosensors, Phys. Rev. A 104 (2021) 012407, http://dx.doi.org/10.1103/PhysRevA.104.012407.
[47] A.Z. Goldberg, A.B. Klimov, M. Grassl, G. Leuchs, L.L. Sánchez-Soto, Extremal quantum states, AVS Quantum Sci. 2 (4) (2020) 044701, http://dx.doi.org/10.1116/5.0025819.
[48] J. Zimba, Anticoherent spin states via the majorana representation, Electron. J. Theor. Phys. 3 (10) (2006) 143–156.
[49] J. Crann, R. Pereira, D.W. Kribs, Spherical designs and anticoherent spin states, J. Phys. A 43 (25) (2010) 255307, http://dx.doi.org/10.1088/1751-8113/43/25/255307.
[50] O. Giraud, D. Braun, D. Baguette, T. Bastin, J. Martin, Tensor representation of spin states, Phys. Rev. Lett. 114 (2015) 080401, http://dx.doi.org/10.1103/PhysRevLett.114.080401.
[51] D. Baguette, F. Damanet, O. Giraud, J. Martin, Anticoherence of spin states with point-group symmetries, Phys. Rev. A 92 (5) (2015) 052333, http://dx.doi.org/10.1103/PhysRevA.92.052333.
[52] C. Chryssomalakos, H. Hernández-Coronado, Optimal quantum rotosensors, Phys. Rev. A 95 (2017) http://dx.doi.org/10.1103/PhysRevA.95.052125.
[53] A.Z. Goldberg, D.F.V. James, Quantum-limited Euler angle measurements using anticoherent states, Phys. Rev. A 98 (2018) 032113, http://dx.doi.org/10.1103/PhysRevA.98.032113.
[54] U. Fano, Geometrical characterization of nuclear states and the theory of angular correlations, Phys. Rev. 90 (4) (1953) 577–579, http://dx.doi.org/10.1103/physrev.90.577.
[55] L. Zhang, Matrix integrals over unitary groups: An application of Schur-Weyl duality, 2015, arXiv:1408.3782 URL https://arxiv.org/abs/1408.3782.